NACA TN 4272 10613

TECH LIBRARY KAFB, NM
0066912

NATIONAL ADVISORY COMMITTEE FOR AERONAUTICS

TECHNICAL NOTE 4272

USE OF THE COANDA EFFECT FOR OBTAINING JET DEFLECTION AND LIFT WITH A SINGLE FLAT-PLATE DEFLECTION SURFACE

By Uwe H. von Glahn

Lewis Flight Propulsion Laboratory
Cleveland, Ohio

Washington
June 1958

AFMDC
TECH

TECH LIBRARY KAFB, NM
0066912

NATIONAL ADVISORY COMMITTEE FOR AERONAUTICS

TECHNICAL NOTE 4272

USE OF THE COANDA EFFECT FOR OBTAINING JET DEFLECTION AND LIFT WITH A SINGLE FLAT-PLATE DEFLECTION SURFACE

By Uwe H. von Glahn

4745

CM-1

SUMMARY

The ratios of lift and axial thrust to undeflected thrust of nozzle-deflection-plate configurations using the Coanda effect for obtaining jet deflection and lift were evaluated from force measurements. Pressure distributions were also obtained over the surface of the deflection plate. The convergent nozzles used in the study were of rectangular cross section with exit heights ranging from 0.5 to 3.7 inches. The deflection surfaces were single flat plates from 1.37 to 11.75 inches long. The nozzles discharged into quiescent air over a range of pressure ratios from 1.5 to 3.0.

In general, the performance of Coanda nozzles is substantially the same as that theoretically calculated for a flat-plate flap immersed in an airstream. For optimum performance, the ratios of lift to undeflected thrust were approximately equal to the sine of the deflection angle; however, the maximum obtainable ratio was angle-limited, depending on nozzle height and pressure ratio. The following table gives orders of magnitude (estimated from data) of the optimum performance for two Coanda nozzles with a plate length of 2.5 inches and at a nominal pressure ratio of 2.1:

Nozzle height, in.	Ratio of lift to undeflected thrust	Ratio of axial to undeflected thrust	Deflection angle, deg
0.5	0.48	0.77	27
2.0	.26	.91	15

For ratios of lift to undeflected thrust equal to theoretical values, pressures less than atmospheric existed over the entire surface of the deflection plate. An empirical relation was developed for predicting the required plate length in terms of the nozzle height for achieving optimum ratio of lift to undeflected thrust at a given deflection-plate angle and pressure ratio.

INTRODUCTION

During the past 15 years considerable attention has been given to aircraft configurations utilizing propeller thrust for vertical lift to support the aircraft at zero ground speed, in order to make a practical vertical takeoff and landing aircraft (VTOL). The areas of usefulness for VTOL and STOL (short takeoff and landing) aircraft have been discussed and evaluated previously (refs. 1 to 4). Within the past two years jet engines with favorable thrust-to-weight ratios have become available. As a result, interest in jet-supported VTOL and STOL aircraft has grown.

14745

Since 1955 the NACA Lewis laboratory has been conducting research on jet-deflection devices for use on VTOL, STOL, and conventional types of turbojet-powered aircraft. The emphasis of the research has been placed on three principal applications of jet-deflection devices: (1) devices that provide jet support for VTOL aircraft oriented in a horizontal attitude with respect to the ground, (2) devices that provide jet directional control forces during takeoff and landing when the airspeed is too low for aerodynamic control surfaces to be effective or during flight at high altitudes where the aerodynamic surfaces also may lose some of their control effectiveness, and (3) devices that augment the lift of the aerodynamic surfaces either during takeoff and landing (STOL aircraft) or at high-altitude cruise. In general, the application of jet deflection for control and lift augmentation requires only partial deflection or turning of the jet; consequently, a large portion of the engine thrust still is available for axial thrust.

As part of its research program on jet-deflection devices the NACA has conducted an exploratory study of the use of the Coanda effect as a means of obtaining vertical lift for jet-powered VTOL and STOL aircraft. The Coanda effect may be described as the phenomenon by which the proximity of a surface to a jet stream will cause the jet to attach itself to and follow the surface contour (ref. 5). When such a surface is placed at an angle to the original jet (or nozzle) axis, the jet stream will be deflected. The local pressures on the deflecting surface are less than ambient air pressure. If the deflecting surface is directed toward the ground, these negative pressures result in a lift component. A drag component constituting a thrust reduction in the axial thrust direction is also obtained. Use of the Coanda effect can be made in studies of the jet flap, vectored slipstream, and supercirculation devices for augmenting the lift of airfoils (refs. 6 and 7).

In the over-all program concerned with the use of the Coanda effect for obtaining jet deflection and vertical lift, the performance characteristics of various deflection-plate shapes were studied, including single flat-plate, multiple flat-plate, and curved-plate configurations.

These data are summarized briefly in reference 8. The study reported herein is concerned with the flow and performance characteristics associated with single flat-plate jet-deflecting surfaces. Empirical relations between nozzle size, deflection-plate length, and deflection-plate angle are presented which yield optimum lift with minimum size of the deflection plate. For convenience and in order to provide flexibility for altering the deflection-plate angle, rectangular nozzles rather than conventional circular nozzles were used. The nozzles were of a simple convergent design, no effort being made to achieve an optimum exhaust-nozzle flow coefficient. The combination of nozzle and jet deflecting surface will hereinafter be called a "Coanda nozzle." The studies were conducted with a small-scale setup (equivalent nozzle-exit diameter less than 2.75 in.) with unheated air and pressure ratios across the nozzle (ratio of absolute jet total pressure to ambient pressure) from 1.5 to 3.0. All data were obtained by discharging the jet into still air at approximately sea-level atmospheric conditions.

4745

CM-1 back

APPARATUS

Test Facility

The test stand shown schematically in figure 1 was used to support the nozzle configurations and to obtain thrust and lift measurements. The test stand consisted of a plenum section (inside diam., 3 in.; length, 16.5 in.) mounted horizontally on a link-supported force-measuring system. Unheated air at approximately 50° F was supplied to the plenum by 2.5-inch-inside-diameter twin supply lines (fig. 2). These lines were placed diametrically opposite one another and at right angles to the plenum in order to eliminate possible side and thrust forces caused by the entering air. These lines were also isolated from the force-measuring system by flexible couplings at each end of the supply lines. A flange to which the nozzles were bolted was provided at the downstream end of the plenum section.

The airflow through the main air supply line was measured and calibrated by means of vertical and horizontal total- and static-pressure probe traverses. From this calibration the pressure indications from a single Pitot-static probe mounted in the center of the supply line were used to determine the magnitude of the airflow during the nozzle tests. A single total-pressure probe mounted just inside the nozzle-exit plane was used to measure the total pressure of the jet stream.

The net thrust obtained with the nozzle configurations was measured by strain gages mounted near the upstream end of the plenum section (fig. 1). The strain gages on the vertical support link under the nozzle flange were used to measure gross values of vertical or lift forces. The force

measurements obtained with these strain gages were recorded on a modified flight recorder.

Coanda Nozzles

A Coanda nozzle (fig. 3) consists of a convergent nozzle exit, deflecting plate, and side plates. The nozzles used herein were formed by flattening progressively a 2.9-inch-inside-diameter tube to a rectangular exit cross section with a desired nozzle height. The exit corners had radii of the order of 0.03 inch. Vertical and horizontal cross sections at the centerlines of the nozzles and pertinent dimensions are presented in figure 4.

4745

The jet-deflection plates, ranging in length from 1.37 to 11.75 inches, were attached to the nozzle by a piano hinge in order to permit rapid changing of the deflection angle between the plates and the nozzle axes. A telescoping-tube mechanism supported the downstream end of the plate. This mechanism was attached to a bracket, which in turn was secured to the nozzle flange. Side plates (figs. 1 and 3) were attached to the jet-deflection plates in order to obtain two-dimensional airflow over the plates. In most cases the height of the side plates was equal to the nozzle height; exceptions to this will be discussed later herein as required. The side plates were sealed to the jet-deflection plate to prevent air leakage onto or away from the deflection plate. Pressure taps were located along the centerline of each jet-deflection plate. For several runs, additional pressure taps were located along the plate length 0.25 inch from each side plate in order to verify the two-dimensional character of the flow.

All pressure data were recorded photographically from multiple-tube manometers.

PROCEDURE

Force and pressure data were obtained over a range of nominal pressure ratios across the nozzles from 1.5 to 3.0. The jet stream discharged into quiescent air at an ambient pressure of 29.2±0.3 inches of mercury.

The forces on a Coanda nozzle and the moment arms are shown in the following sketch:

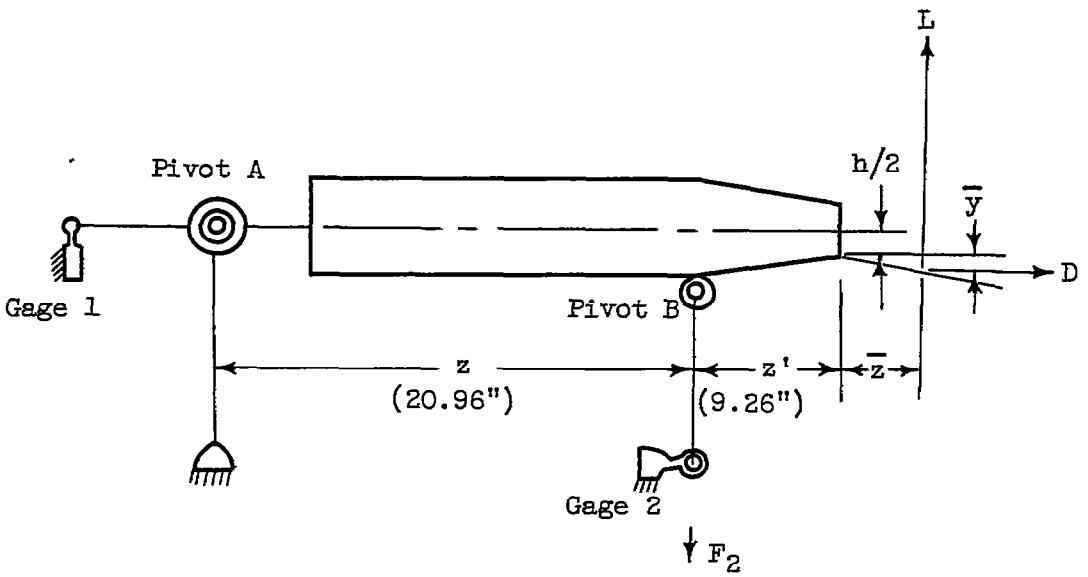

(All symbols used herein are defined in appendix A.) It was determined that the horizontal force measurements were independent of any vertical force; hence, the axial thrust was obtained directly from strain gage 1. The moment about pivot A consisted of two components, the lift caused by the deflection plate and the axial-thrust reduction (drag) caused by the plate. In order to calculate the net lift, moments about pivot A were found from the following equations:

$$L(z + z' + \bar{z}) + D\left(\frac{h}{2} + \bar{y}\right) = F_2(z) \tag{1}$$

or

$$L = \frac{F_2(20.96) - D\left(\frac{h}{2} + \bar{y}\right)}{(30.22 + \bar{z})} \tag{2}$$

The thrust-reduction force (drag of deflection plate) D was calculated by subtracting the measured axial thrust obtained with the deflected plate from that obtained with the undeflected jet (no deflection plate). The values of $\bar{y}$ and $\bar{z}$ were obtained from center-of-pressure calculations based on the pressure distribution over the deflection plate. Values of $\bar{z}$ were considered positive when the center of pressure was

located to the right of the nozzle exit, and values of $\bar{y}$ were considered positive when the center of pressure was below the lower lip of the nozzle exit.

In general, the deflection-plate angle for a particular Coanda nozzle was set at a predetermined value, and all pressure and force data were recorded as the nominal pressure ratio was increased progressively from 1.5 to 3.0. Data recording generally was terminated for any particular configuration when the deflection-plate angle was sufficiently large to cause jet-stream detachment from the plate. This jet-stream detachment was observed visually; sufficient water vapor condensed out of the air leaving the nozzle to permit easy visualization of the jet stream. At the same time that jet detachment was observed, the lift force was reduced, the axial thrust was increased to values approaching the undeflected thrust, and the local surface pressures on the deflection plate approached the ambient pressure. The deflection-plate angle was accurate to $\pm 0.25^{\circ}$ while the airflow was turned off. However, with progressively increasing pressure ratios the deflection angle at high lifts (associated with deflection angles greater than 20°) could change as much as 1.5° less than the nominal measured angle because of slack in the hinge and telescoping support tube.

The nozzle-plate combinations and conditions studied are summarized in the following table:

Nozzle height, h, in.	Nominal pressure ratio, P_N/p_0	Plate length, l, in.	Deflection-plate angle, θ, deg
0.5	1.5,1.8, 2.1,2.7, 3.0	1.37,2.5, 3.5,6.5, 11.75	10 to 38
1.1	1.5,1.8, 2.1,2.7, 3.0	2.5,3.5, 6.5,11.75	10 to 35
2.0	1.5,1.8, 2.1,2.7	2.5,3.5, 11.75	10 to 30
3.7	1.5,1.8, 2.1	7.0	10 to 20

RESULTS AND DISCUSSION

Over-All Performance

The performance of each Coanda nozzle is evaluated in terms of the ratios of lift and axial thrust to the jet thrust obtained from each nozzle without a deflection plate (undeflected thrust).

Nozzle thrust coefficients with undeflected jet. - In terms of the ratio of undeflected thrust for a test nozzle to the theoretical thrust of a circular nozzle of equal flow area (nozzle thrust coefficient), the following values were obtained over the range of pressure ratios studied:

Nozzle height, h, in.	Approximate nozzle thrust coefficient
0.5	0.97
1.1	.91
2.0	.87
3.7	.91

As will be shown later, the performance of the Coanda configuration using the nozzle with a nozzle coefficient of 0.97 does not differ significantly from that with a coefficient of 0.87.

Performance of Coanda nozzles. - The performance of the Coanda nozzles in terms of the ratio of lift to undeflected thrust $\mathscr{F}_L$ and the ratio of axial to undeflected thrust $\mathscr{F}_Z$ (hereinafter called axial-thrust ratio) as functions of deflection-plate angle is presented in table I. Cross plots of these data show that the performance ($\mathscr{F}_L$ and $\mathscr{F}_Z$) for a particular configuration at a given deflection angle is substantially independent of pressure ratio as long as jet detachment from the deflection plate does not occur. Consequently, the discussion of the data in this section will be confined to a pressure ratio of 2.1, and the trends of the data will be considered representative of those occurring at the other pressure ratios studied.

The variation of the ratio of lift to undeflected thrust and the axial-thrust ratio for nozzle heights of 0.5, 1.1, and 2.0 inches are shown in figure 5 as a function of deflection-plate angle θ. Data are presented for plates varying in length from 2.5 to 11.75 inches. As a basis for comparison, the theoretical performance characteristics of a flat-plate flap immersed in an airstream (ref. 9) are also presented in figure 5. The theoretical $\mathscr{F}_L$ values for such a flap are equal to the

4745

sine of the deflection-plate angle, while the theoretical $\mathscr{F}_z$ values are represented by the following equation:

$$\mathscr{F}_z = 1 - \sin\theta \tan\theta \qquad (3)$$

Figure 5 shows that the experimental $\mathscr{F}_L$ values increase with progressively increasing deflection-plate angle θ to a maximum value depending on plate length and nozzle height. Beyond the maximum values, $\mathscr{F}_L$ decreases with increasing deflection angle because of partial jet detachment from the deflection plate. The data show that in many cases for a particular deflection angle and no jet detachment a short deflection plate relative to the nozzle height will attain near theoretical $\mathscr{F}_L$ values (sine curve), whereas progressively longer plates will attain $\mathscr{F}_L$ values progressively lower than theoretical values. For example, in figure 5(b) a comparison of the $\mathscr{F}_L$ values at a deflection angle of 20° for the 3.5-, 6.5-, and 11.75-inch-long deflection plates shows that $\mathscr{F}_L$ values of 0.36, 0.30, and 0.30, respectively, are obtained. The decrease in $\mathscr{F}_L$ values with increasing plate length for a given deflection angle is caused by an undesirable pressure distribution over the downstream portion of the longer plates that reduces the lift, as discussed in appendix B.

Further examination of the $\mathscr{F}_L$ data in figure 5 also shows that a long plate generally can be deflected to a larger angle than a short plate before jet detachment from the plate occurs. The maximum $\mathscr{F}_L$ value attainable with a long plate may exceed that obtainable with a short plate; however, the fact that $\mathscr{F}_L$ values of progressively longer plates fall increasingly below the sine curve indicates a reduced performance, as previously discussed.

The data in figure 5 show that some of the $\mathscr{F}_L$ values for deflection-plate lengths of 2.5 and 3.5 inches fall above the sine curve. This is not considered particularly significant and could result from inaccuracies inherent in the test setup or from small amounts of thrust augmentation that may be obtainable with a Coanda nozzle (ref. 10). These data, therefore, should be considered as indicating only that efficiencies near theoretical can be obtained with a Coanda nozzle.

The axial-thrust ratios $\mathscr{F}_z$ in figure 5 decrease with progressively increasing deflection angle and are in good agreement with the theoretical curve (eq. (3)) if jet detachment from the deflection plate does not occur. Incipient or partial jet detachment is indicated when the axial-thrust ratio is larger than the value of the theoretical curve, an $\mathscr{F}_z$ value of

1.0 indicating complete jet detachment. No effects due to varying the deflection-plate length for a particular Coanda nozzle are observed in the data except those affecting jet detachment from the deflection plate.

Miscellaneous performance characteristics. - As part of the study reported herein, a brief test was conducted to determine the effect of nozzle aspect ratio on the performance of a Coanda nozzle having a specified nozzle height. (Nozzle aspect ratio is defined as the ratio of nozzle width to height at the exit.) For this test a splitter plate the same height as the nozzle exit was mounted longitudinally on a deflection plate midway between the side plates. In this manner the nozzle aspect ratio was effectively halved. For the nozzle used in this test (h, 0.5 in.), the measured lift and thrust reduction were the same as those for the configuration without the splitter plate.

Only limited and inconclusive data were obtained on the effect of side-plate height on the performance of a Coanda nozzle. The data showed that side plates were required to obtain maximum $\mathscr{F}_L$ values and delay jet detachment. The erratic nature of the data can be illustrated by the fact that a reduction in side-plate height to 25 percent of the nozzle height for the 0.5-inch nozzle did not cause appreciable changes in the lift compared with a side-plate height equal to the nozzle height; however, a reduction in side-plate height to 50 percent of the nozzle height for the 2.0-inch nozzle caused considerable reductions in the lift and partial jet detachment. No effect on lift was observed when the side-plate height exceeded that of the nozzle height (by up to 100 percent). Consequently, the data reported herein were obtained with side-plate heights equal to or somewhat greater than the nozzle height and equal in length to the deflection plate.

In an evaluation of over-all performance characteristics of the Coanda nozzles several practical aspects also are of interest. It was determined that air leaks between the side plates and the deflection plate can cause jet detachment, especially if the leak occurs near a region of high negative pressures on the plate surface. On the other hand, air leaks between the side plates and nozzle exit or between the deflection plate and the nozzle exit were not detrimental to the configuration performance. Slots at the junction of the nozzle exit and the deflection plate (caused by the hinge), which were about 0.06 inch deep and 0.1 inch wide and ran the width of the nozzle, were not detrimental to the performance.

Comparison of Vertical Lift Obtained with Coanda Nozzle with That for Other Jet-Deflection Devices

In evaluating the vertical-lift capability of a Coanda nozzle, it is of interest to compare its performance with that of some other deflection

4745 CM-2

devices. Reference 9 presents performance data at a pressure ratio of 2.0 for a number of jet-deflection devices including (1) swivel nozzles, tailpipes, and shrouds; (2) internal and external flaps; and (3) auxiliary-bleed nozzles at 90° to the tailpipe. In terms of the variation of deflected-force ratio (herein $\mathscr{F}_L$) with axial-thrust ratio, these devices can be compared by the use of the three theoretical performance curves shown in figure 6. The swivel-nozzle devices follow the "cosine law" variation of $\mathscr{F}_L$ with $\mathscr{F}_Z$ (ref. 9). The flap devices, including the Coanda nozzles, follow the sine curve for $\mathscr{F}_L$ and equation (3) for $\mathscr{F}_Z$. The performance of the auxiliary-bleed nozzle follows a linear relation of the amount of flow bled through the auxiliary nozzle to that through the primary nozzle, and thus $\mathscr{F}_L$ varies directly with $\mathscr{F}_Z$.

4745

Many of the devices, including the Coanda nozzle (with single flat-plate deflection surface), internal and external flaps, swivel primary nozzle, and so forth, may have aerodynamic or mechanical limitations, or both, to the amounts of lift that can be achieved and are therefore more applicable for horizontal attitude STOL than for VTOL. It is therefore desirable to maintain a large value of $\mathscr{F}_Z$ as well as to achieve a maximum $\mathscr{F}_L$. From this consideration it can be seen that the deflection devices represented by the flap-type deflectors (including the Coanda nozzles) compare reasonably well for moderate deflection forces with the devices that follow the cosine law, the latter being considered herein as optimum deflection devices. For example, at an $\mathscr{F}_L$ value of 0.30 the optimum $\mathscr{F}_Z$ value is about 0.95 compared with about 0.91 for a flap-type deflector. At the same $\mathscr{F}_L$ value, the auxiliary-bleed nozzle had an $\mathscr{F}_Z$ value of only 0.70. At large values of $\mathscr{F}_L$ the comparison becomes less favorable. For the flap-type deflectors, however, it should be pointed out that the $\mathscr{F}_Z$ values at large values of $\mathscr{F}_L$ can be improved through the use of multiple flat-plate or curved-plate deflection surfaces as discussed in reference 8. Further discussion of these improvements is beyond the scope of this study.

Generalization of Data for Optimum Performance

A study of the force and pressure-distribution data showed several trends that appeared amenable to generalization of the data. In particular, an effort was made to determine the relation of the deflection-plate length to the nozzle height for achieving theoretical $\mathscr{F}_L$ values (sine curve, fig. 5) for a given pressure ratio and deflection-plate angle. It should be noted that the theoretical $\mathscr{F}_L$ values given by the sine curve are independent of plate length; however, the experimental $\mathscr{F}_L$

values are closely related to the physical dimensions of a particular combination of nozzle and deflection plate. Because of the limited number of Coanda nozzles studied, the parameters used in correlating the data may apply directly only over the range of conditions studied herein. These parameters may change for a more complete range of variables that would include greater changes in nozzle-exit design, heated air, and so forth. Also, because of the small scale of the models, the pressure gradients and Reynolds numbers associated with full-scale nozzles may affect the results presented herein.

4745

CM-2 back

Pressure distribution. - The pressure distribution over the deflection plate of a Coanda nozzle consisted of two primary types shown in the following sketch and denoted as optimum and nonoptimum:

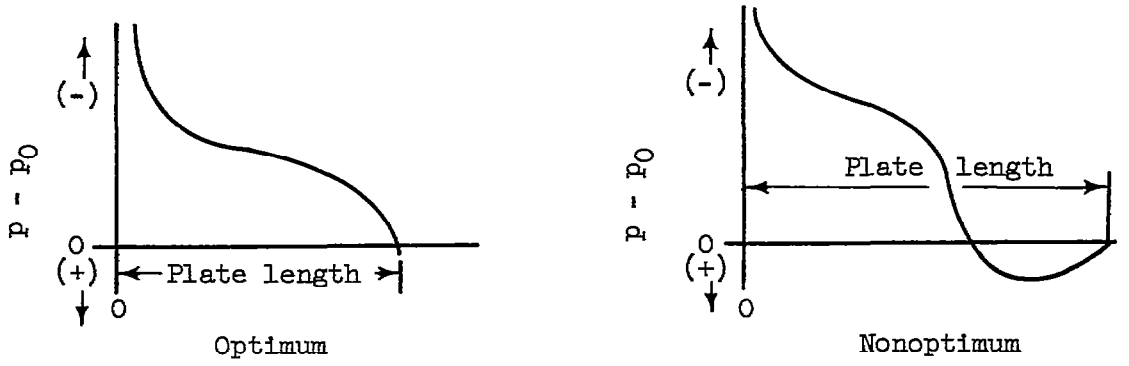

The pressure distributions in this sketch are shown in terms of the difference between the local surface pressure p and the ambient pressure p_0 as a function of surface distance along the deflection plate measured from the nozzle exit l'. The optimum pressure distribution is characterized by negative pressure values (local surface pressures less than ambient) over the entire length of the deflection plate. The nonoptimum pressure distribution is characterized by negative pressure values over the plate surface near the nozzle exit followed by positive pressure values on the downstream portion of the deflection plate. It should be noted that, for a given flow condition, the pressure distribution upstream of the zero pressure location is independent of the plate length and of pressures downstream of this point. Details of the pressure distribution over the deflection plates of the Coanda nozzles studied herein are discussed in appendix B.

A study of the measured force and pressure-distribution data showed that theoretical $\mathscr{F}_L$ values were obtained only when the local surface pressures were negative over essentially the entire length of the deflection plate (see also appendix B). If the initial location of the zero pressure coefficient (local surface pressure equal to ambient pressure)

coincides with the downstream end of the deflection plate, the maximum $\mathscr{F}_L$ value (equal to or slightly greater than theoretical $\mathscr{F}_L$) for a particular Coanda nozzle is obtained together with the maximum deflection angle for the plate. A further increase in the deflection angle results in jet detachment and a reduction in $\mathscr{F}_L$. A decrease in deflection angle for such a configuration precludes jet detachment but initiates positive pressures on the downstream portions of the deflection plate. As the extent of the positive pressures increases with progressively decreasing angles (nonoptimum pressure distribution), the $\mathscr{F}_L$ values become considerably less than the theoretical $\mathscr{F}_L$ values. For a configuration with zero pressure coefficient at the downstream end of the plate, jet detachment occurs if the plate length is reduced.

Study of the data also shows that, above a critical deflection angle (discussed in the following paragraphs) for a particular nozzle height, theoretical $\mathscr{F}_L$ values cannot be obtained regardless of plate length or deflection angle, the pressure distribution always being nonoptimum.

Plate length necessary for theoretical $\mathscr{F}_L$ values. - From the foregoing considerations and appendix B, it is postulated that the location of the zero pressure coefficient (obtained from the pressure distribution data) defines the minimum plate length (optimum) required to yield theoretical $\mathscr{F}_L$ values for a particular nozzle height and a specified deflection-plate angle below the critical angle. In figure 7 the length of the deflection plate upstream of the location of the initial zero pressure coefficient l_{opt} is plotted as a function of the deflection angle for a nozzle height of 1.1 inches and a nominal pressure ratio of 2.1. The plate length necessary to obtain theoretical $\mathscr{F}_L$ values is seen to increase with increasing deflection angle. The curve is terminated at about 27° (critical deflection angle), because the local pressures and force data for this nozzle height and pressure ratio showed that, with deflection angles greater than 27°, optimum pressure distributions and theoretical $\mathscr{F}_L$ values could not be obtained. With plate lengths greater than that given for a deflection angle of 27°, deflection angles greater than the critical angle can be achieved; however, the resultant $\mathscr{F}_L$ value, although possibly a maximum $\mathscr{F}_L$, will be less than that which theoretically could be obtained at the supercritical deflection angle. Use of optimized multiple flat plates or a curved plate is suggested as a more efficient means of achieving deflection angles greater than the critical angle associated with a given single flat-plate configuration.

Critical deflection angles for which theoretical $\mathscr{F}_L$ values could be obtained are shown in figure 8 as a function of nozzle height for all

4745

pressure ratios studied. These data show that with increasing nozzle height theoretical $\mathscr{F}_L$ values are obtained for progressively lower ranges of deflection angles. Figure 8 also shows that, for the range of conditions and configurations covered, the data are apparently independent of pressure ratio.

Data-correlation parameter. - In generalizing the data, an empirical relation was developed in which, for each pressure ratio, the ratio of the plate length necessary for achieving theoretical $\mathscr{F}_L$ values (optimum plate length l_{opt}) to the nozzle height raised to an exponential power was obtained as a function of deflection-plate angle. This ratio, l_{opt}/h^n, is shown in figure 9 as a function of θ for nominal pressure ratios of 1.5, 1.8, 2.1, 2.7, and 3.0. Also shown in figure 9 are the critical deflection angles below which theoretical $\mathscr{F}_L$ values are obtained for the nozzle heights of 0.5, 1.1, and 2.0 inches. It is apparent from the curves in figure 9 that l_{opt}/h^n increases with progressively increasing deflection angle.

The exponent n was determined to be a function of the deflection-plate angle and pressure ratio and could be expressed as

$$n = -a\theta + b \tag{4}$$

where a and b must be determined for each pressure ratio. The values of a and b determined for the pressure ratios studied herein are plotted as a function of pressure ratio in figure 10. A reversal of the resulting curves occurred near the choking limit and precluded a simple general solution over the entire range of pressure ratios.

The following example illustrates the use of figures 8 to 10. It is desired to determine the plate lengths required for theoretical $\mathscr{F}_L$ values for a nozzle height of 1.5 inches over a range of deflection-plate angles and pressure ratios from 1.5 to 3.0. The data in figure 8 indicate that the maximum deflection-plate angle (critical) that can be used to obtain theoretical $\mathscr{F}_L$ values is near 25°. From figure 9 the required l_{opt}/h^n for deflection-plate angles of 10°, 15°, 20°, and 25° can be obtained for pressure ratios of 1.5, 1.8, 2.1, 2.7, and 3.0. The appropriate value of n for the l_{opt}/h^n parameter is determined by use of figure 10, and the value of l_{opt} is then calculated. The results of these calculations are shown in figure 11 as a plot of plate length against pressure ratio for the specified deflection-plate angles. It is evident from figure 11 that relatively large plate lengths with respect to nozzle height are required to achieve theoretical $\mathscr{F}_L$ values at large deflection-plate angles. The generalization of the location of the zero

4745

pressure coefficient by the use of the nozzle height raised to the exponent n suggested that a similar generalization, within limits, might extend to the entire pressure distribution. Such a generalization of the local pressure data is shown in appendix C.

Location of Center of Pressure on Deflection Plate

The location of the lifting force and thrust-reduction force relative to the point of attachment of the deflection plate to the nozzle exit may be of importance for certain pitching or trim considerations. The moment arms $\bar{z}$ and $\bar{y}$ for the lift force and the thrust-reduction force, respectively (see sketch in PROCEDURE), are listed also in table I for all configurations and test conditions. In general, when the extent of negative pressure coefficients was very small compared to the over-all plate length, the effective lift force was located upstream of the nozzle exit and the thrust reduction force was located between the jet axis and the lower surface of the nozzle (negative moments). When the negative pressure coefficients extended over most or all of the plate surface, the lift and thrust-reduction forces were located downstream of the exit nozzle and below the lower nozzle-exit lip, respectively (positive moments).

A simple expression for $\bar{y}$ and $\bar{z}$ in terms of nozzle height, deflection-plate angle, and deflection-plate length is presented in appendix D.

The trim or pitching moments caused by the asymmetrical location of the lift and thrust-reduction forces could be handled readily by an appropriate reaction control device.

CONCLUDING REMARKS

The results of this study have shown that properly designed Coanda nozzles utilizing a single flat plate for deflecting the jet stream yield vertical lift of the same order of magnitude as that calculated theoretically for a flat plate or a flap immersed in an airstream. The ratio of lift to undeflected thrust for such Coanda nozzles is approximately equal to the sine of the deflection-plate angle.

The practical use of a Coanda nozzle with a single flat-plate deflection surface appears to be limited to STOL rather than VTOL aircraft because of jet detachment from the deflection surface at large deflection angles. The angle to which the jet stream can be deflected by a Coanda nozzle depends primarily on the nozzle height, plate length, and pressure ratio. For example, with nozzle heights of 0.5 and 2.0 inches and a deflection-plate length of 2.5 inches, maximum ratios of lift to undeflected thrust near 0.48 (deflection angle, 27°) and 0.26 (deflection

angle, approximately 15°) and axial-thrust ratios of 0.77 and 0.92, respectively, were obtained at a nominal pressure ratio of 2.1. In order to obtain a jet-stream deflection of the order of 90° for VTOL, multiple flat-plate or curved-plate configurations rather than a single flat-plate configuration must be used (ref. 8).

Because the deflection surfaces are necessarily large to achieve good performance and a high degree of jet-stream turning for STOL or VTOL aircraft, best utilization of a Coanda nozzle can be achieved by designing an aircraft with due consideration of the unique characteristics of the device rather than attempting to incorporate the device in an existing configuration.

Lewis Flight Propulsion Laboratory
National Advisory Committee for Aeronautics
Cleveland, Ohio, March 19, 1958

APPENDIX A

SYMBOLS

D	deflection-plate drag force, lb
F	force measured by strain-gage system at location noted, lb
F_j	undeflected jet thrust (no deflection plate), lb
$\mathscr{F}_L$	ratio of lift to undeflected thrust, L/F_j
$\mathscr{F}_Z$	ratio of axial thrust with deflection plate to undeflected thrust (also called axial-thrust ratio)
h	nozzle height, in.
L	vertical lift, lb
l	total length of deflection plate, in.
l'	surface distance measured from nozzle exit to a point on deflection plate, in.
P_j	jet total pressure, in. Hg gage
P_N	jet total pressure, in. Hg abs
p	local static pressure on deflection plate, in. Hg abs
p_O	atmospheric pressure, in. Hg abs
$\bar{y}$	vertical location of center of pressure referenced to lower lip of nozzle exit, in.
$\bar{z}$	horizontal location of center of pressure referenced to nozzle-exit plane, in.
z,z'	horizontal lever arms, in.
θ	deflection-plate angle, deg

Subscript:

opt	optimum

APPENDIX B

PRESSURE DISTRIBUTION OVER DEFLECTION PLATES

Order of magnitude and trends of specific effects on the pressure distribution over the deflection plate due to pressure ratio, plate length, deflection angle, and nozzle height are discussed in the following sections. The data shown in the accompanying figures are presented in terms of a local surface pressure coefficient $(p - p_0)/P_j$ as a function of surface distance measured along the plate surface from the nozzle exit l'. Because the ambient pressure varied by only 1 percent for these studies, gage values of jet total pressure P_j are used for convenience rather than absolute pressures. The data shown in the subsequent figures are considered representative of all the Coanda nozzle configurations studied herein. Also, except as noted, the discussions will be concerned with that portion of the deflection plates subject only to negative surface pressure coefficients.

Effect of Pressure Ratio on Local Surface Pressure Coefficients

Typical profiles of pressure distributions above and below choking conditions are shown in figure 12. The data shown are for pressure ratios of 1.8 and 2.7, nozzle height of 1.1 inches, deflection-plate angle of 10°, and several plate lengths. In general, for a pressure ratio below choking, the local surface pressure coefficients decreased as a smooth curve with increasing distance from the nozzle exit, reaching a zero pressure coefficient at some distance from the exit; thereafter, the coefficients became positive. For pressure ratios above choking, a double-peak profile of negative pressure coefficients generally was obtained, the first peak occurring near the nozzle exit and the second some distance downstream of the nozzle exit. After the second peak the pressure coefficients decreased and became positive farther downstream on the plate. Several small regions of negative pressure may occur and alternate with regions of positive pressure on the downstream portions of the deflection plate. These small regions of negative pressure are believed to have been caused by impingement on the plate of local shock waves existing in the jet stream at pressure ratios well above those required for choked flow.

Effect of Deflection-Plate Length

The local pressure coefficients over the deflection plate for a particular Coanda nozzle (fig. 12) are substantially independent of plate length if the jet stream is attached to the plate surface. When jet

detachment occurs, the negative pressure coefficients are reduced (negative pressures approach ambient pressure value) compared with those for which the jet stream is attached to the deflection plate.

Plate length had substantially no effect on the negative pressures on the upstream surface of the plate. Therefore, a plate with its length terminated at the zero-pressure-coefficient location should yield the maximum and theoretical $\mathscr{F}_L$ value for a given nozzle height, deflection-plate angle, and pressure ratio. That is, no positive pressures exist on the plate to reduce its lift capability. This maximum $\mathscr{F}_L$ value is equal to or exceeds the theoretical $\mathscr{F}_L$ value, as demonstrated in the following example. Consider figure 13, in which the local surface pressure coefficients over an 11.75-inch and a 3.5-inch plate are plotted as a function of surface distance along the plate (nozzle height, 1.1 in.; nominal pressure ratio, 3.0; deflection-plate angle, 20°). The zero pressure coefficient is located about 3.3 inches from the nozzle exit. This location is nearly at the end of the 3.5-inch plate, and negative pressure coefficients exist over essentially the entire plate. The experimental $\mathscr{F}_L$ value for the 3.5-inch plate was 0.38 compared with the theoretical value of 0.342; whereas the $\mathscr{F}_L$ value for the 11.75-inch plate was 0.27. Because the location of zero pressure coefficient is slightly before the end of the 3.5-inch plate, it is to be expected that this plate could be deflected 2° or 3° more in order to obtain the maximum and theoretical $\mathscr{F}_L$ value for this configuration. A deflection of the plate to 25° resulted in jet detachment and a loss in $\mathscr{F}_L$. Limited data are available for the case in which the location of zero pressure coefficient coincides approximately with the end of the plate. These data show that a maximum $\mathscr{F}_L$ value equal to or slightly greater than theoretical is obtained (circle symbol at a deflection angle of 15°, fig. 5(c), is such a point).

4745

Effect of Deflection-Plate Angle

With increasing deflection-plate angle the zero pressure coefficient occurs at progressively larger distances from the nozzle exit, as shown in figure 14(a) (nozzle height, 1.1 in.; nominal pressure ratio, 2.1; plate length, 11.75; deflection-plate angles, 10°, 15°, 20°, and 25°). An increase in deflection angle may initially increase the local negative pressure coefficients near the nozzle exit (see square and circle symbols); however, after a particular deflection angle is reached (depending also on the pressure ratio), the local negative pressure coefficients near the nozzle exit are reduced, as shown by the diamond and triangle symbols. Integrating the area under the pressure-distribution curve (and also force measurements) showed that the increased region of negative pressures obtained with the larger deflection angles more than offsets the decrease

in local pressures near the nozzle exit. As a result, the lift normal to the deflection-plate surface increases progressively with increasing deflection angle until jet detachment occurs.

Effect of Nozzle Height

An increase in the nozzle height (larger mass flow per unit nozzle width) caused the pressure field to extend progressively farther downstream on the deflection plate, as shown in figure 14(b). (The data shown in this figure are for nozzle heights of 0.5, 1.1, and 2.0 in.; deflection-plate angle of 15°; and nominal pressure ratio of 2.1.) The location of the zero pressure coefficient therefore moves progressively downstream with increasing nozzle height. For example, in figure 14(b) the zero pressure coefficients occur at about 0.8, 1.6, and 2.6 inches from the nozzle exit for nozzle heights of 0.5, 1.1, and 2.0 inches, respectively.

4745 CM-3 back

APPENDIX C

CORRELATION OF PRESSURE DISTRIBUTION IN TERMS OF RATIO OF LOCAL SURFACE DISTANCE TO NOZZLE HEIGHT RAISED TO n-POWER

The local negative pressure coefficients over the deflection plate, shown as a function of the ratio of local surface distance from the nozzle exit l' to h^n in figure 15, include only data obtained without the occurrence of jet detachment from the plate surface. The data are shown for nozzle heights of 0.5, 1.1, and 2.0 inches and are presented in order of increasing deflection-plate angles and pressure ratio. The data generally correlate well for deflection-plate angles up to and including 20°. At deflection angles greater than 20° some data scatter is apparent, which increases with progressively increasing deflection angles.

Pressure coefficients as a function of l'/h^n for the nozzle with a height of 3.7 inches are presented separately in figure 16 because of the pressure-profile changes on the deflection plate caused by the contour of the nozzle exit (nozzle lip). Nozzles that have an abrupt lip (see fig. 4; nozzle heights of 0.5, 1.1, and 2.0 in.) generally cause higher negative pressure coefficients to occur on the deflection plate near the nozzle exit than a nozzle with a relatively flat lip (see fig. 4; nozzle height 3.7 in.). Use of the latter nozzle causes the peak negative pressure coefficients to occur farther downstream on the plate than use of the former nozzles. However, the variation of $\mathscr{F}_L$ and $\mathscr{F}_z$ with θ and the location of the zero pressure coefficient do not appear to be affected by the change in nozzle-lip shape.

4745

APPENDIX D

CENTER-OF-PRESSURE LOCATION ON DEFLECTION PLATE

An empirical equation for $\bar{y}$ and $\bar{z}$ was derived in terms of the nozzle height, deflection-plate angle, and over-all plate length. A simple expression of these relations is given by the following equations:

$$\left.\begin{aligned} \bar{y} &= -\frac{cl^{m}}{h^{n}} + e\theta \\ \bar{z} &= -\frac{fl^{m'}}{h^{n}} + g\theta \end{aligned}\right\} \qquad (D1)$$

where c, e, f, g, m, and m' are constants that must be determined for each pressure ratio from cross plots of the data in table I.

For a pressure ratio of 2.1 equation (D1) yields the following:

$$\left.\begin{aligned} \bar{y} &= -\frac{0.40l^{0.42}}{h^{n}} + 0.05\ \theta \\ \text{and} \\ \bar{z} &= -\frac{0.57l^{0.60}}{h^{n}} + 0.1\ \theta \end{aligned}\right\} \qquad (D2)$$

The exponent n is obtained from equation (4). Experimental moment arms are plotted against values calculated from equation (D2) in figure 17. These data are for nozzle heights of 0.5, 1.1, and 2.0 inches, plate lengths of 2.5, 3.5, 6.5, and 11.75 inches, and deflection-plate angles from 10° up to those associated with maximum $\mathscr{F}_L$ ratios for each configuration. Generally good agreement is observed between the experimental data and the calculated data.

It is of interest to consider the practical application of these data. Consider a Coanda nozzle with a height of 1 inch operating at a pressure ratio of 2.1. Assume that the deflection plate can be constructed so that (1) at each deflection-plate angle the plate length results in the theoretical $\mathscr{F}_L$ value, or (2) the plate length is fixed to yield the theoretical $\mathscr{F}_L$ value only at the maximum angle. In the latter case decreasing the deflection angle results in positive pressures progressively covering more of the plate surface starting at the downstream

end of the plate. The locations of the effective forces are summarized in the following table:

Deflection-plate angle, θ, deg	Plate length, l, in.	$\bar{z}$, in.	$\bar{y}$, in.	$\bar{z}$, in.	$\bar{y}$, in.
		Variable l (equal to l_{opt} at each angle)		l = 3.5 in.	
10	1.10	0.40	0.08	-0.20	-0.18
15	1.55	.76	.27	.30	.07
20	2.30	1.05	.42	.70	.32
25	3.50	1.30	.57	1.30	.57

At deflection-plate angles less than the maximum (25°), the forces are located nearer the nozzle exit and jet axis when the plate length used is longer than l_{opt} for a particular deflection angle. Equation (D1) applies strictly only to the configurations used in the analysis (nozzle heights, 0.5, 1.1, and 2.0 in.), since they are functions of the pressure distribution over the deflection plate. However, the changes in $\bar{y}$ and $\bar{z}$ caused by a difference in the pressure distribution over the plate such as shown in figure 16 for a nozzle height of 3.7 inches should not affect $\bar{y}$ and $\bar{z}$ appreciably.

REFERENCES

1. Zimmerman, Charles H.: Some General Considerations Concerning VTOL Aircraft. SAE Jour., vol. 64, no. 8, July 1956, pp. 68-74.

2. Garbell, M. A.: Technical Aspects of Steep-Gradient Aircraft. Interavia, vol. XI, no. 1, Jan. 1956, pp. 27-34.

3. Woodham, R. M.: Safety Through Steep Gradient Aircraft. The Daniel & Florence Guggenheim Aviation Safety Center, Cornell Univ., May 1956.

4. Meyerhoff, Leonard, and Meyerhoff, Stanley: Reverse Thrust, Vertical Lift, and Jet Side Force by Means of Controlled Jet-Deflection. TN 56-168, Eastern Research Group, Jan. 1956. (Contract AF-18(600)-1530.)

5. Metral, Albert R.: Method of Increasing Fluid Stream by Diverting It from Its Axis of Flow. Coanda Effect. Trans. Rep. No. F-TS-823-RE, WADC-AMC, Feb. 1948.

6. Kuhn, Richard E., and Draper, John W.: Investigation of Effectiveness of Large-Chord Slotted Flaps in Deflecting Propeller Slipstreams Downward for Vertical Take-Off and Low-Speed Flight. NACA TN 3364, 1955.

7. Kuhn, Richard E., and Spreemann, Kenneth P.: Preliminary Investigation of the Effectiveness of a Sliding Flap in Deflecting a Propeller Slipstream Downward for Vertical Take-Off. NACA TN 3693, 1956.

8. von Glahn, Uwe H., and Povolny, John H.: Considerations of Some Jet-Deflection Principles for Directional Control and for Lift. Preprint No. 219, SAE, 1957.

9. McArdle, Jack G.: Internal Characteristics and Performance of Several Jet Deflectors at Primary-Nozzle Pressure Ratios up to 3.0. NACA TN 4264, 1958.

10. von Kármán, Theodore: Theoretical Remarks on Thrust Augmentation. Reissner Anniversary Volume, Contributions to Appl. Mech., J. W. Edwards, 1949, pp. 461-468.

TABLE I. - SUMMARY OF PERFORMANCE CHARACTERISTICS OF COANDA NOZZLES[a]

(a) Nozzle height, 0.5 inch

Plate length, 2.5 in.

Deflection angle, δ, deg	Pressure ratio, p_N/p_0	Ratio of lift to undeflected thrust, $\mathcal{F}_L$	Axial-thrust ratio, $\mathcal{F}_x$	$\bar{y}$, in.	$\bar{x}$, in.
10	1.50	0.126	0.949	-0.11	-0.63
	1.81	.144	.913	-.08	-.08
	2.10	.145	.838	-.07	-.43
	2.70	.157	.847	-.05	-.34
	3.02	.142	.960	-.03	-.19
15	1.50	0.232	0.863	-0.01	0.01
	1.80	.229	-----	-.05	-.19
	2.11	.227	.918	-.06	-.19
	2.70	.257	.817	.02	.10
	3.02	.215	.923	.05	.20
20	1.50	0.318	0.903	0.04	0.12
	2.11	.310	.887	.02	.05
	2.70	.308	.880	.07	.19
	3.01	.323	.872	.13	.33
25	1.50	0.450	0.828	0.30	0.67
	1.81	.426	.788	.36	.77
	2.11	.443	.786	.35	.74
	2.69	.426	.794	.31	.66
	3.01	.441	.780	.33	.71
27	2.13	0.485	0.788	0.36	0.70
	2.72	.478	.755	.38	.74
	3.01	.492	.719	.34	.67
[c]15	1.82	0.244	0.961	0.02	-0.09
	2.10	.263	-----	.02	.05
	2.70	.234	.928	.06	.30
[c]20	1.79	0.308	0.918	0.04	0.11
	2.69	.303	.888	.17	.48
	3.02	.308	.874	.27	.73
[c]25	1.81	0.390	0.848	0.32	0.67
	2.69	.346	.826	.33	.73
	3.01	.366	.827	.34	.71

Plate length, 3.5 in.

Deflection angle, δ, deg	Pressure ratio, p_N/p_0	Ratio of lift to undeflected thrust, $\mathcal{F}_L$	Axial-thrust ratio, $\mathcal{F}_x$	$\bar{y}$, in.	$\bar{x}$, in.
20	1.50	0.319	0.887	-0.07	-0.17
	1.81	.311	.847	-.08	-.22
	2.06	.321	.912	-.06	-.15
	2.70	.294	.838	.04	.12
	3.00	.299	.841	.21	.58
25	1.52	0.384	0.830	0.12	0.28
	1.83	.374	.803	.19	.42
	2.10	.376	.792	.19	.41
	2.71	.385	.782	.17	.37
	2.99	.374	.782	.19	.41
30	1.51	0.469	0.744	0.40	0.69
	1.80	.474	.705	.58	.91
	2.11	.506	.679	.64	1.19
	2.72	.500	.730	.68	1.17

Plate length, 6.5 in.

Deflection angle, δ, deg	Pressure ratio, p_N/p_0	Ratio of lift to undeflected thrust, $\mathcal{F}_L$	Axial-thrust ratio, $\mathcal{F}_x$	$\bar{y}$, in.	$\bar{x}$, in.
20	1.52	0.317	0.888	-0.65	-1.79
	1.81	.298	.874	-.48	-1.27
	2.10	.297	.870	-.35	-.97
	2.68	.302	.868	.01	.05
	3.02	.289	.862	.19	.56
30	1.52	0.484	0.729	-0.08	-0.16
	2.11	.427	.742	.23	.45
	2.69	.443	.758	.07	.15
35	1.51	0.493	0.711	0.11	0.14
	1.83	.478	.680	.06	.09
	2.11	.488	.679	.30	.44
	2.68	.509	.792	.61	.87
	3.00	.510	.640	.79	1.22
38	1.49	[b]0.501	0.641	0.16	0.22
	1.79	.510	.610	.37	.46
	2.10	.516	.584	.64	.80
	2.69	.534	.591	.87	1.11
	3.02	[b].515	.602	.96	1.22

Plate length, 11.75 in.

Deflection angle, δ, deg	Pressure ratio, p_N/p_0	Ratio of lift to undeflected thrust, $\mathcal{F}_L$	Axial-thrust ratio, $\mathcal{F}_x$	$\bar{y}$, in.	$\bar{x}$, in.
20	2.71	0.317	0.854	-0.98	-2.82
	3.01	.289	.854	-.33	-.93
25	1.81	0.371	0.817	-0.88	-1.87
	2.13	.371	.822	-.64	-1.37
	2.72	.374	.807	-.65	-1.36
	3.03	.371	.802	-.44	-.95
30	1.51	0.422	0.752	-0.57	-0.74
	1.80	.424	.680	-.43	-.75
	2.09	.401	.651	-.35	-.57
	2.69	.429	.726	-.36	-.69
	3.03	.433	.748	-.48	-.83
35	1.51	0.471	0.680	0	0.02
	1.82	.474	.695	-.10	-.21
	2.11	.470	.718	-.14	-.24
	2.71	.468	.677	-.04	-.02
	3.03	.478	----	-.19	-.31

[a]Performance for nozzle height of 3.7 inches not included because data obtained were primarily information on pressure distribution over deflection plate. Performance data for nozzle height of 0.5 inch and plate length of 1.37 inches not included for the same reason.

[b]Partial or complete jet detachment from deflection plate.

[c]Side-plate height, 0.28 times nozzle height.

TABLE I. - Continued. SUMMARY OF PERFORMANCE CHARACTERISTICS OF COANDA NOZZLES[a]

(b) Nozzle height, 1.1 inches

Deflection angle, θ, deg	Pressure ratio, p_N/p_0	Ratio of lift to undeflected thrust, $\mathcal{F}_L$	Axial-thrust ratio, $\mathcal{F}_x$	$\bar{y}$, in.	$\bar{x}$, in.	Pressure ratio, p_N/p_0	Ratio of lift to undeflected thrust, $\mathcal{F}_L$	Axial-thrust ratio, $\mathcal{F}_x$	$\bar{y}$, in.	$\bar{x}$, in.	Pressure ratio, p_N/p_0	Ratio of lift to undeflected thrust, $\mathcal{F}_L$	Axial-thrust ratio, $\mathcal{F}_x$	$\bar{y}$, in.	$\bar{x}$, in.	Pressure ratio, p_N/p_0	Ratio of lift to undeflected thrust, $\mathcal{F}_L$	Axial-thrust ratio, $\mathcal{F}_x$	$\bar{y}$, in.	$\bar{x}$, in.
	Plate length, 2.5 in.					Plate length, 3.5 in.					Plate length, 8.5 in.					Plate length, 11.75 in.				
10	1.80 2.10 2.66 2.99	0.165 .158 .223 .180	0.996 .905 .974 .959	0.08 .11 .16 .16	0.43 .19 .93 .93	1.51 1.80 2.11 2.69 3.00	0.144 .142 .138 .140 .151	0.994 .991 .978 .972 .962	-0.02 -.02 -.06 -.04 .13	-0.18 -.16 -.37 -.24 .74	1.54 1.78 2.08 2.68 3.04	0.143 .159 .159 .143 .147	0.942 .972 .944 .959 .965	-0.16 -.17 ----- -.12 -.17	-0.94 -.86 ----- -.74 -.67					
15	1.53 1.80 2.13 2.70 2.99	0.264 .265 .269 .253 .207	0.874 .959 .949 .943 .950	0.16 .18 .14 .19 .20	0.59 .64 .51 .69 .73	1.51 1.81 2.10 2.69 3.02	0.225 .222 .216 .220 .260	0.971 .961 .952 .942 .919	0.05 .09 0 .11 .28	0.17 .35 0 .41 1.06	1.51 1.81 2.10 2.69 2.95	0.213 .213 .217 .232 .244	0.967 .935 .928 .928 .928	-0.07 -.05 -.06 .03 0	-0.03 -.14 -.19 .13 -.03					
20	1.50 2.11 2.68	[b]0.147 [b].090 [b].088	0.993 .990 .994	0.32 .33 .32	0.68 .90 .85	1.52 1.80 2.12 2.68 2.98	0.341 .352 .358 .344 .380	0.909 .878 .877 .870 .852	0.29 .36 .37 .29 .42	0.81 .99 1.02 .77 1.15	1.50 2.11 2.69 2.99	0.300 .302 .309 .304	0.912 .885 .878 .875	-0.01 .09 .01 .07	0.04 .23 .03 .21	1.51 1.80 2.11 2.69 3.01	0.297 .292 .300 .305 .290	0.900 .879 .883 .848 .846	-0.26 -.37 -.35 -.39 -.17	-0.56 -1.05 -.97 -1.07 -.39
22.25											1.51 1.80 2.11 2.57 2.97	0.374 .388 .389 .398 .376	0.854 .830 .819 .822 .822	0.18 .19 .32 .40 .19	0.32 .48 .70 .84 .43					
22.5						2.08 2.68 3.01	0.417 .394 .407	0.858 .849 .825	0.51 .38 .49	1.23 .93 1.18										
24.5						1.51 1.81	0.439 .461	0.813 .818	0.47 .57	1.05 1.26										
30											1.51 1.81 2.12 2.68 3.00	0.449 .459 .455 [b].378 [b].393	0.782 .750 .729 .756 .769	0.38 .58 .77 1.08 1.12	0.64 .97 1.30 1.86 1.80	1.51 2.11 2.69 3.00	0.418 .411 .415 .393	0.775 .764 .768 .767	-0.12 .20 .40 .54	-0.24 .40 .77 .94
33																1.52 1.81 2.12 2.69 3.01	0.454 .450 .425 [b].331 [b].268	0.739 .722 .723 .793 .826	0.15 .25 .59 1.23 1.39	0.20 .37 .78 1.99 2.21
35																1.51 1.81 2.03	[b]0.447 [b].441 [b].377	0.698 .711 .748	0.58 .67 1.16	0.79 .89 1.64
[d]15	1.51 1.78 2.10 2.67 2.99	0.212 .204 .209 .192 .175	0.992 .986 .976 .959 .952	0.16 .17 .17 .18 .19	0.60 .64 .63 .70 .73															

[a]Performance for nozzle height of 3.7 inches not included because data obtained were primarily information on pressure distribution over deflection plate. Performance data for nozzle height of 0.5 inch and plate length of 1.57 inches not included for the same reason.

[b]Partial or complete jet detachment from deflection plate.

[d]No side plates.

TABLE I. - Concluded. SUMMARY OF PERFORMANCE CHARACTERISTICS OF COANDA NOZZLES[a]

(c) Nozzle height, 2.0 inches

Deflection angle, θ, deg	Pressure ratio, P_N/P_0	Ratio of lift to undeflected thrust, $\mathcal{F}_L$	Axial-thrust ratio, $\mathcal{F}_z$	$\bar{y}$, in.	$\bar{z}$, in.	Pressure ratio, P_N/P_0	Ratio of lift to undeflected thrust, $\mathcal{F}_L$	Axial-thrust ratio, $\mathcal{F}_z$	$\bar{y}$, in.	$\bar{z}$, in.	Pressure ratio, P_N/P_0	Ratio of lift to undeflected thrust, $\mathcal{F}_L$	Axial-thrust ratio, $\mathcal{F}_z$	$\bar{y}$, in.	$\bar{z}$, in.
	Plate length, 2.5 in.					Plate length, 3.5 in.					Plate length, 11.75 in.				
10	1.49	0.162	0.992	0.11	0.62	1.51	0.147	-----	0.10	0.58	1.52	0.145	0.968	-0.06	0
	1.81	.160	.973	.08	.47	1.82	.147	-----	.06	.36	0.81	.136	.953	-.17	-.97
	2.12	.182	.970	.11	.62	2.12	.149	0.966	.05	.27	2.12	.145	.945	-.21	-1.44
	2.69	.170	.941	.23	1.29						2.70	.150	-----	-.35	-.83
12.5	1.52	0.185	0.988	0.17	0.75										
	1.82	.195	.939	.14	.63										
	2.13	.237	.927	.18	.81										
	2.72	.181	.951	.26	1.16										
	2.31	.252	.939	.22	.96										
15	1.53	0.221	0.988	0.24	0.90	1.50	0.247	0.992	0.25	0.91					
	1.80	[b].177	.972	.26	.98	1.82	.249	.954	.26	.96					
	2.12	.258	.914	.22	.82	2.12	.262	.958	.21	.78					
	2.70	[b].190	.972	.25	.97	2.70	.270	.967	.38	1.41					
20	1.52	[b]0.126	0.944	0.40	1.10	1.51	0.377	0.934	0.45	1.24	1.82	0.304	0.873	0.28	0.77
	1.83	[b].089	.943	.42	1.16	1.83	[b].216	.963	.52	1.43	2.12	.290	.831	.15	.40
	2.13	[b].080	.955	.42	1.13	2.12	.360	-----	.54	1.48	2.69	.286	.875	.27	.81
	2.69	[b].181	.947	.36	.99										
	2.83	[b].180	.944	.28	.77										
22.5						1.52	[b]0.182	0.944	0.59	1.42					
						1.81	[b].142	.975	.63	1.51					
						2.11	[b].118	.977	.62	1.49					
						2.72	[b].124	-----	.62	1.49					
25						1.50	[b]0.142	0.965	0.68	1.46	1.52	0.376	0.840	0.57	1.24
						1.81	[b].116	.963	.69	1.46	1.83	.367	.829	.62	1.34
						2.11	[b].100	.982	.71	1.52	2.13	.362	.832	.68	.74
											2.68	.328	.847	.46	.96
27.5											1.51	[b]0.392	0.901	0.77	1.53
											1.81	.448	.814	.96	1.89
											2.13	[b].339	.822	1.07	2.04
											2.71	[b].335	.856	.72	1.59
30											1.51	[b]0.368	0.788	1.11	1.97
											1.83	[b].324	.816	1.21	2.15
											2.13	[b].298	.835	1.32	2.24
											2.69	[b].269	.842	1.38	2.38

[a]Performance for nozzle height of 3.7 inches not included because data obtained were primarily information on pressure distribution over deflection plate. Performance data for nozzle height of 0.5 inch and plate length of 1.37 inches not included for same reason.

[b]Partial or complete jet detachment from deflection plate.

4745
CM-4 back

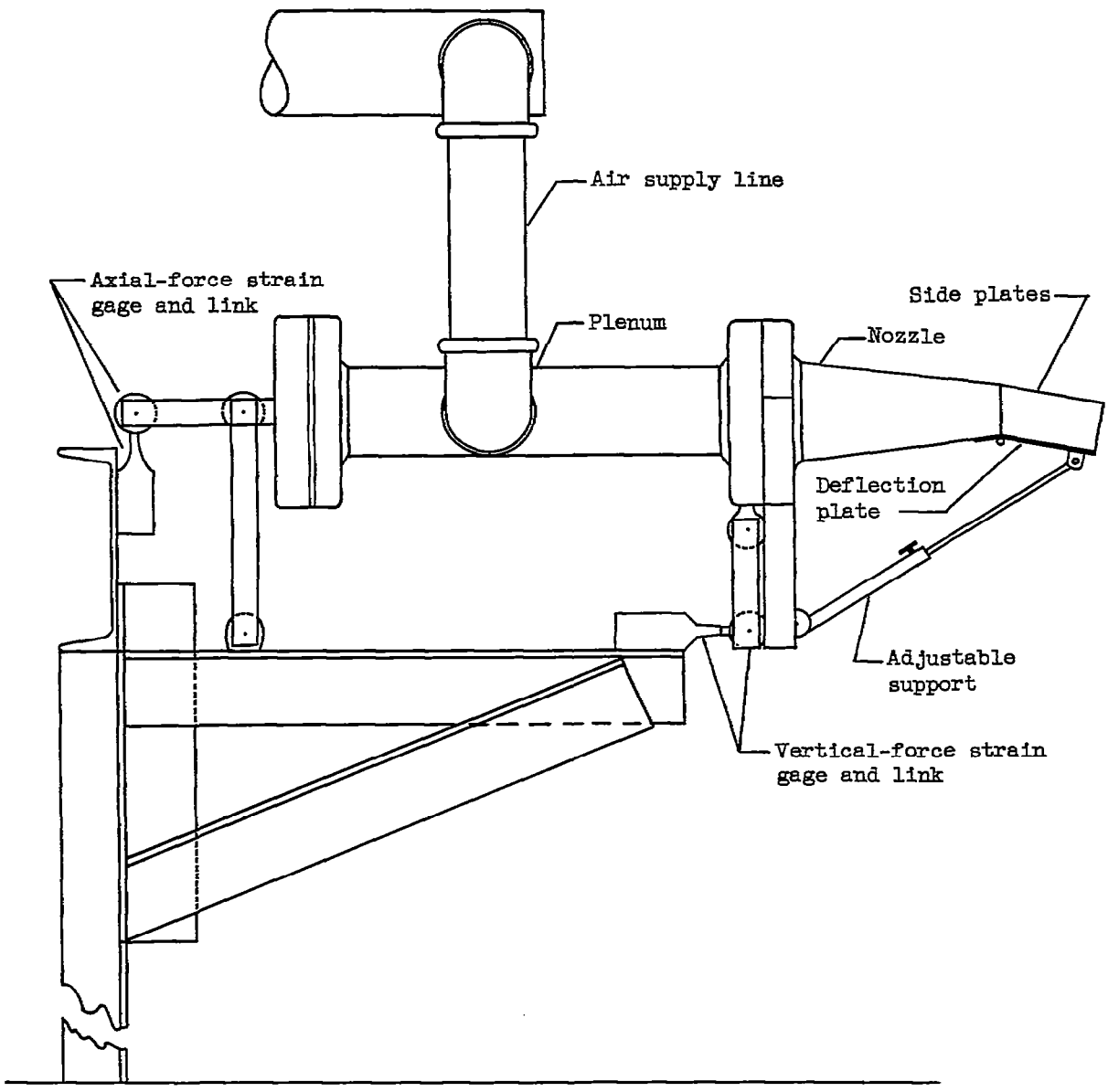

Figure 1. - Setup for Coanda nozzle tests.

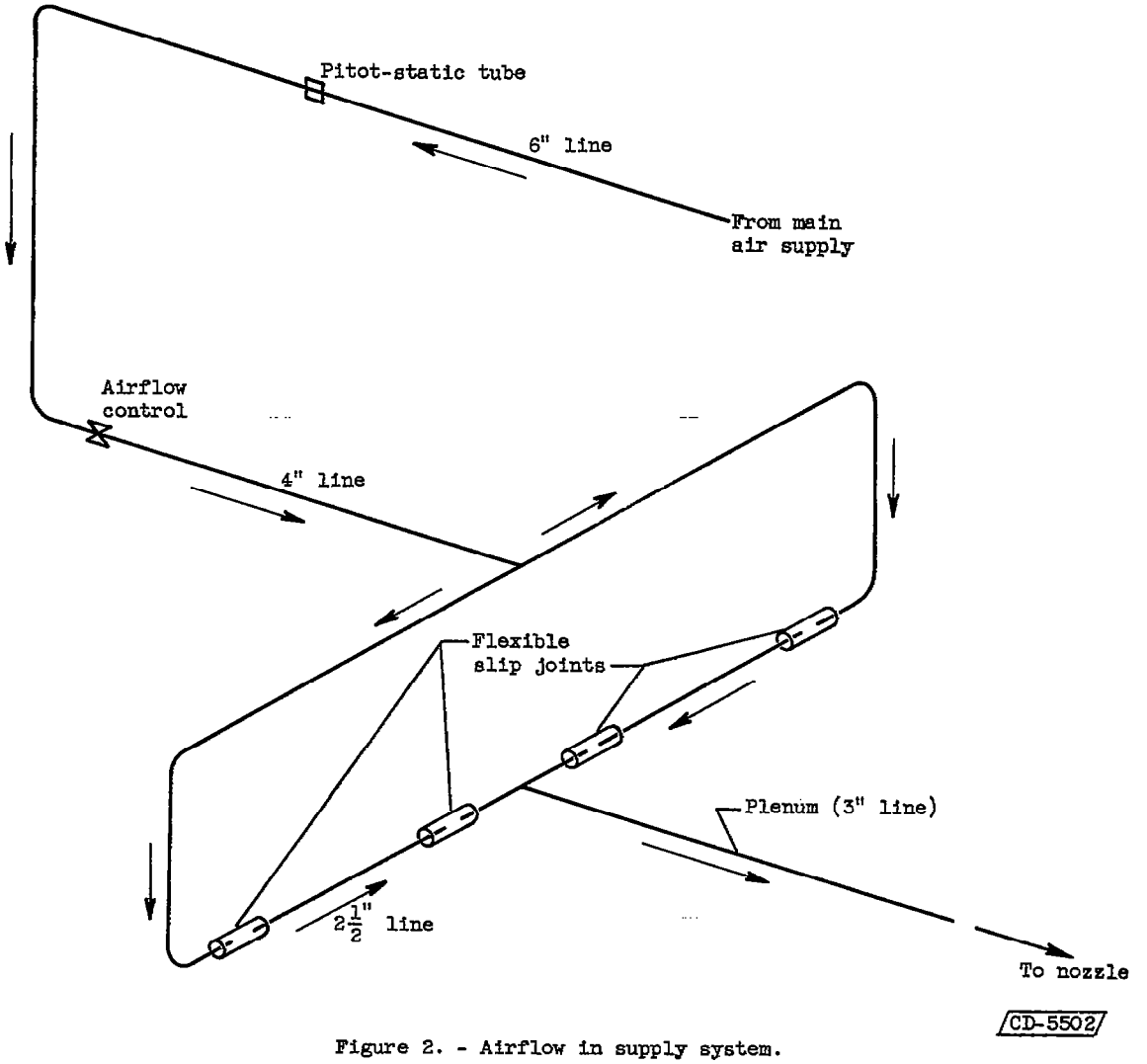

Figure 2. - Airflow in supply system.

4745

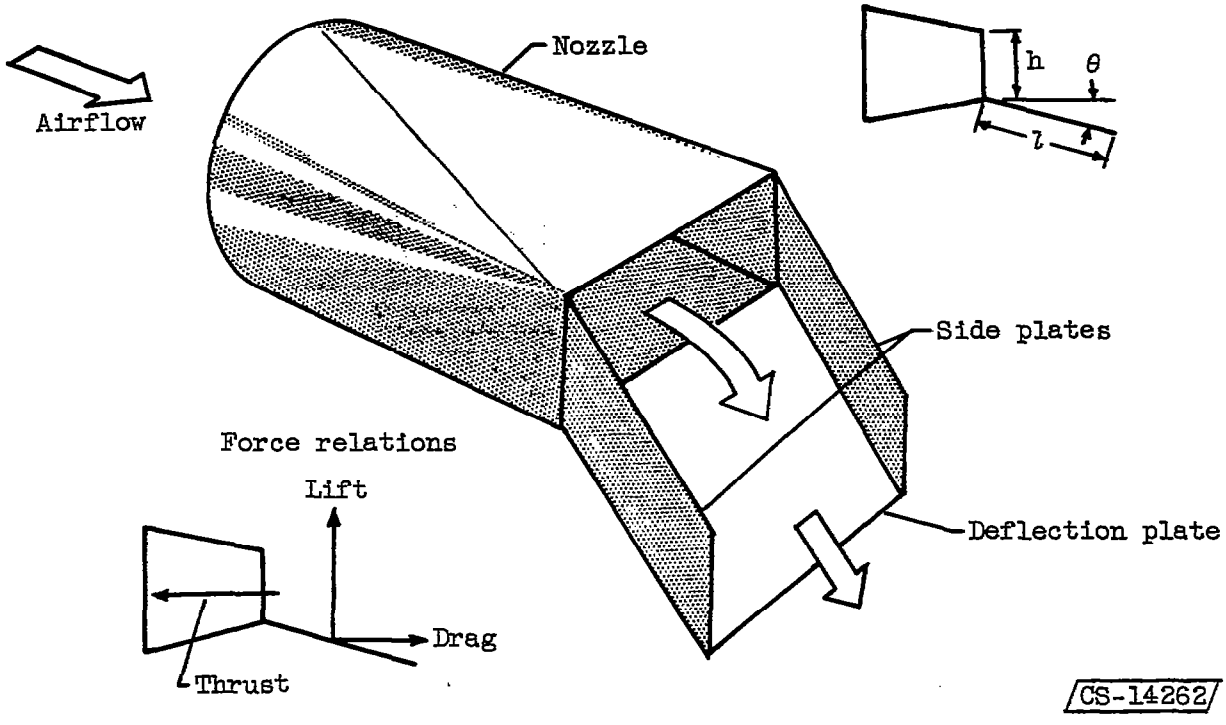

Figure 3. - Coanda nozzle using single flat plate for jet deflection.

Nozzle	Height, in.	Width, in.	Exit area, sq in.
A	0.5	4.2	2.1
B	1.1	3.7	4.1
C	2.0	2.8	5.6
D	3.7	1.1	4.1

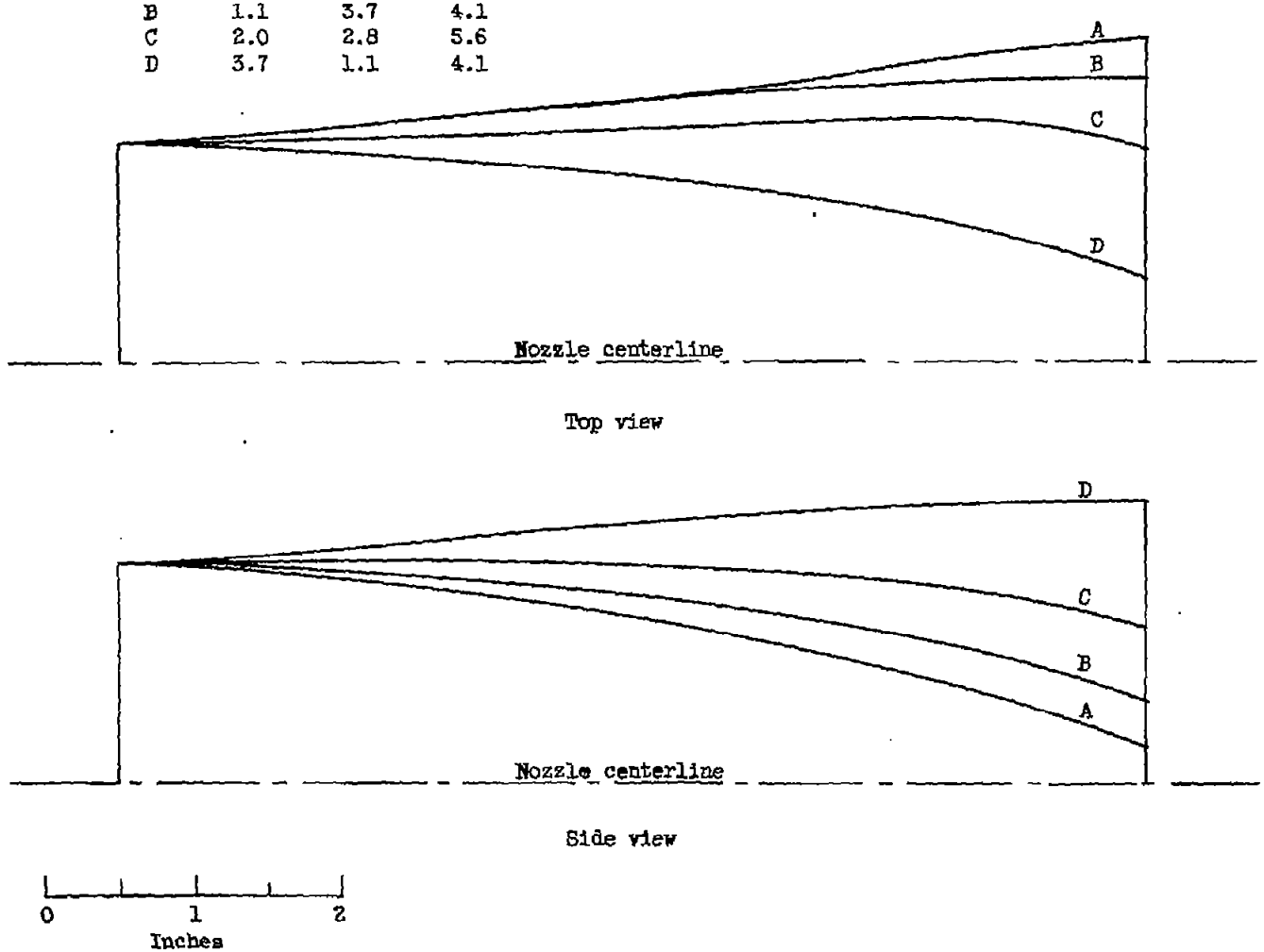

Figure 4. - Cross sections of nozzles.

4745

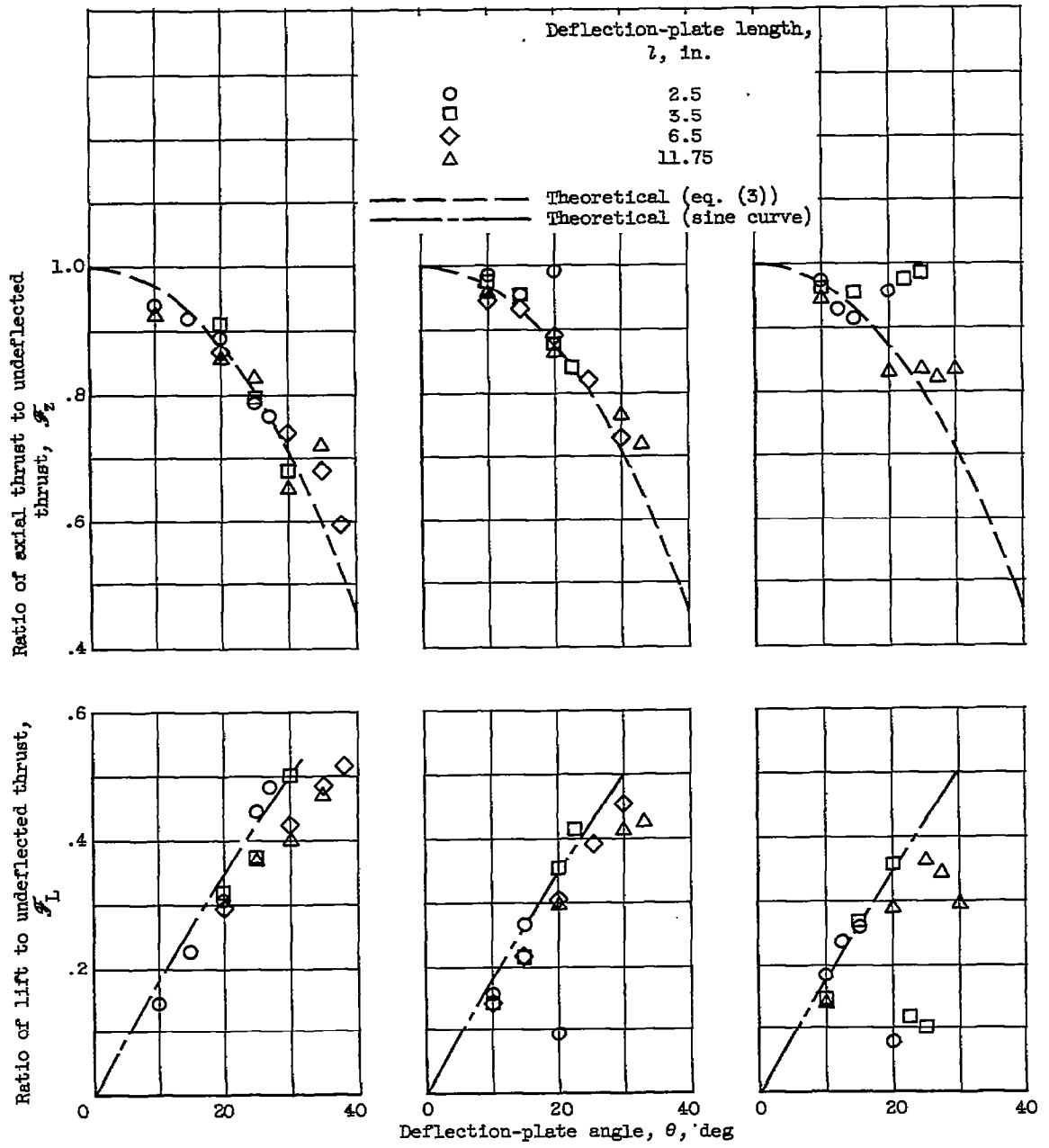

(a) Nozzle height, 0.5 inch.

(b) Nozzle height, 1.1 inches.

(c) Nozzle height, 2.0 inches.

Figure 5. - Typical performance of Coanda nozzles as function of deflection-plate angle. Nominal pressure ratio, 2.1.

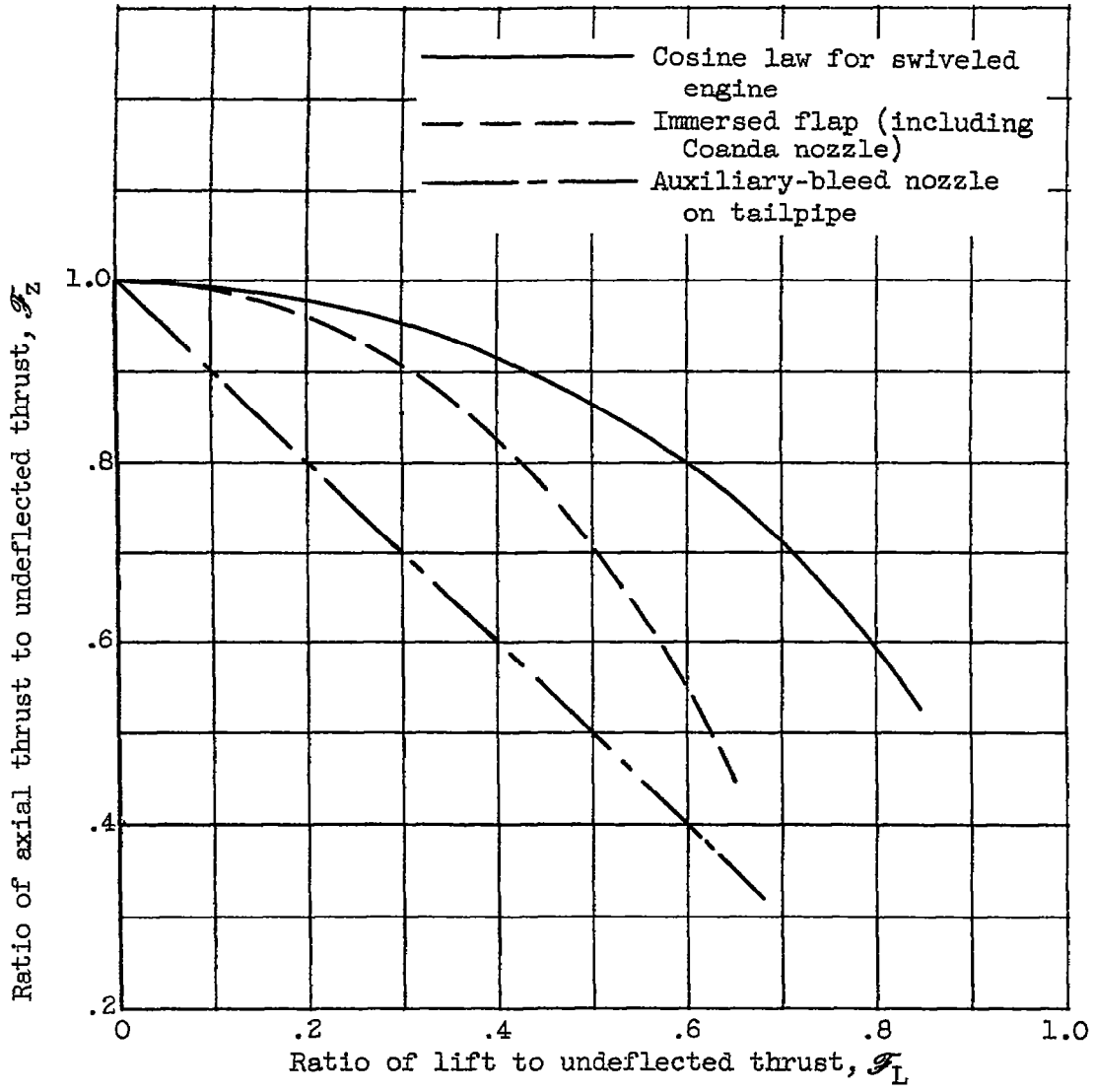

Figure 6. - Analytical performance comparison of several types of jet-stream deflection devices (ref. 9).

4745

4745 CM-5

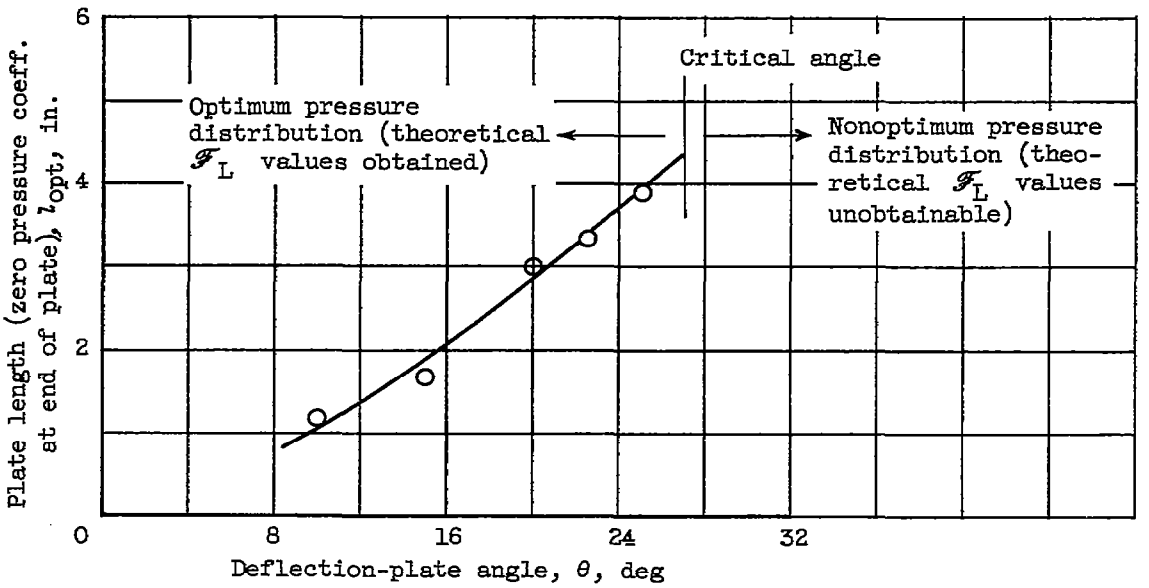

Figure 7. - Minimum plate lengths required to obtain theoretical $\mathcal{F}_L$ values as function of deflection-plate angle. Nozzle height, 1.1 inches; nominal pressure ratio, 2.1.

4745

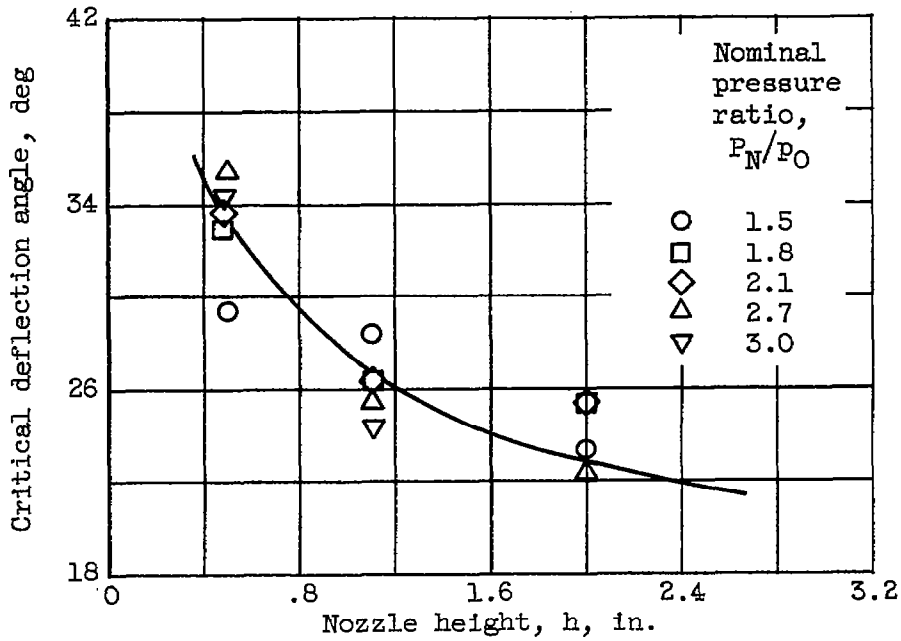

Figure 8. - Variation of critical deflection-plate angle below which theoretical $\mathcal{F}_L$ values can be obtained with nozzle height.

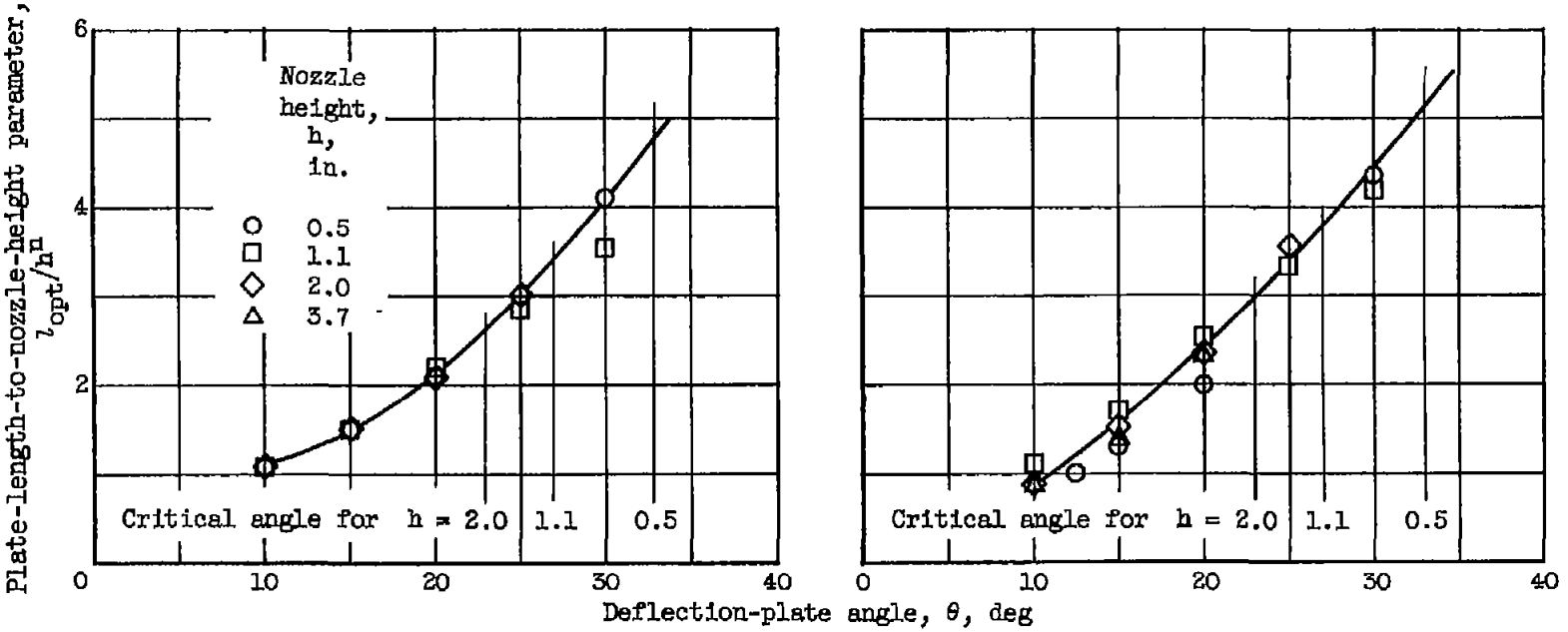

(a) Pressure ratio, 1.5; $n = -0.0108\theta + 1.11$.

(b) Pressure ratio, 1.8; $n = -0.0195\theta + 1.22$.

Figure 9. - Correlation of plate-length-to-nozzle-height parameter with deflection-plate angle for theoretical ratio of lift to undeflected thrust.

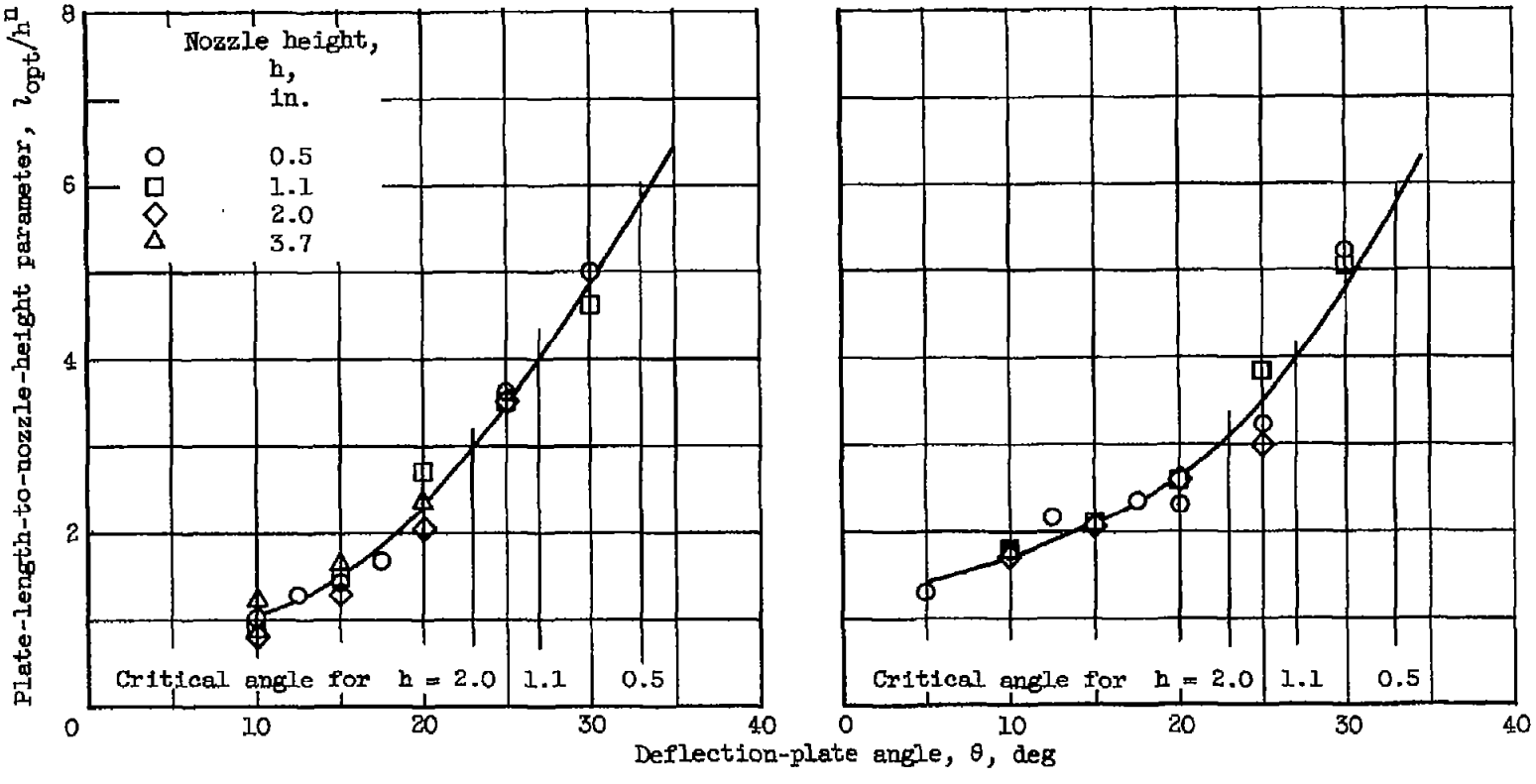

(c) Pressure ratio, 2.1; $n = -0.0136\theta + 1.10$.

(d) Pressure ratio, 2.7; $n = -0.0070\theta + 0.795$.

Figure 9. - Continued. Correlation of plate-length-to-nozzle-height parameter with deflection-plate angle for theoretical ratio of lift to undeflected thrust.

4745

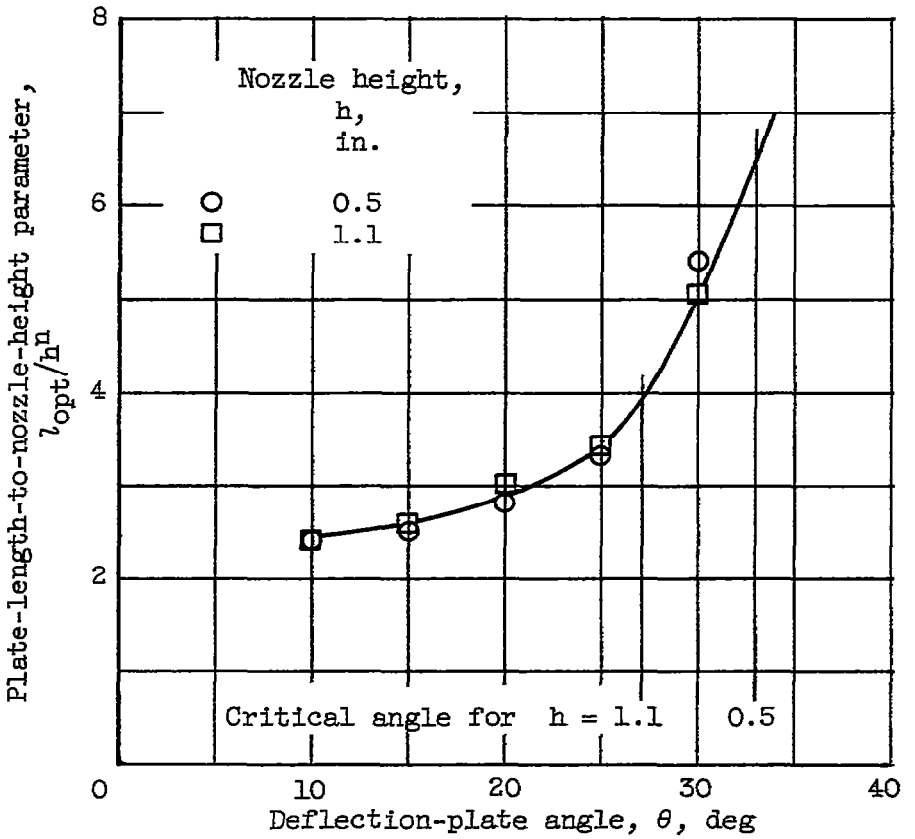

(e) Pressure ratio, 3.0; $n = -0.0053\theta + 0.760$.

Figure 9. - Concluded. Correlation of plate-length-to-nozzle-height parameter with deflection-plate angle for theoretical ratio of lift to undeflected thrust.

4745

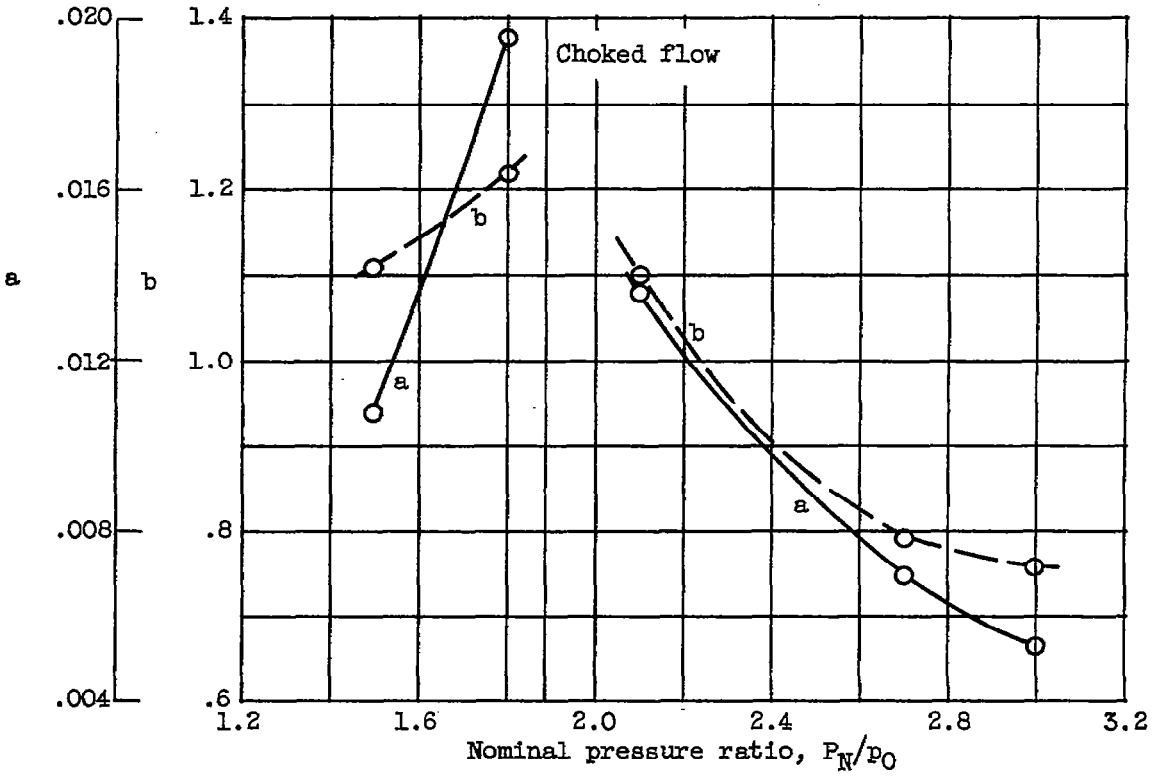

Figure 10. - Variation of exponent constants in plate-length-to-nozzle-height parameter l_{opt}/h^n with pressure ratio. $n = -a\theta + b$.

4745

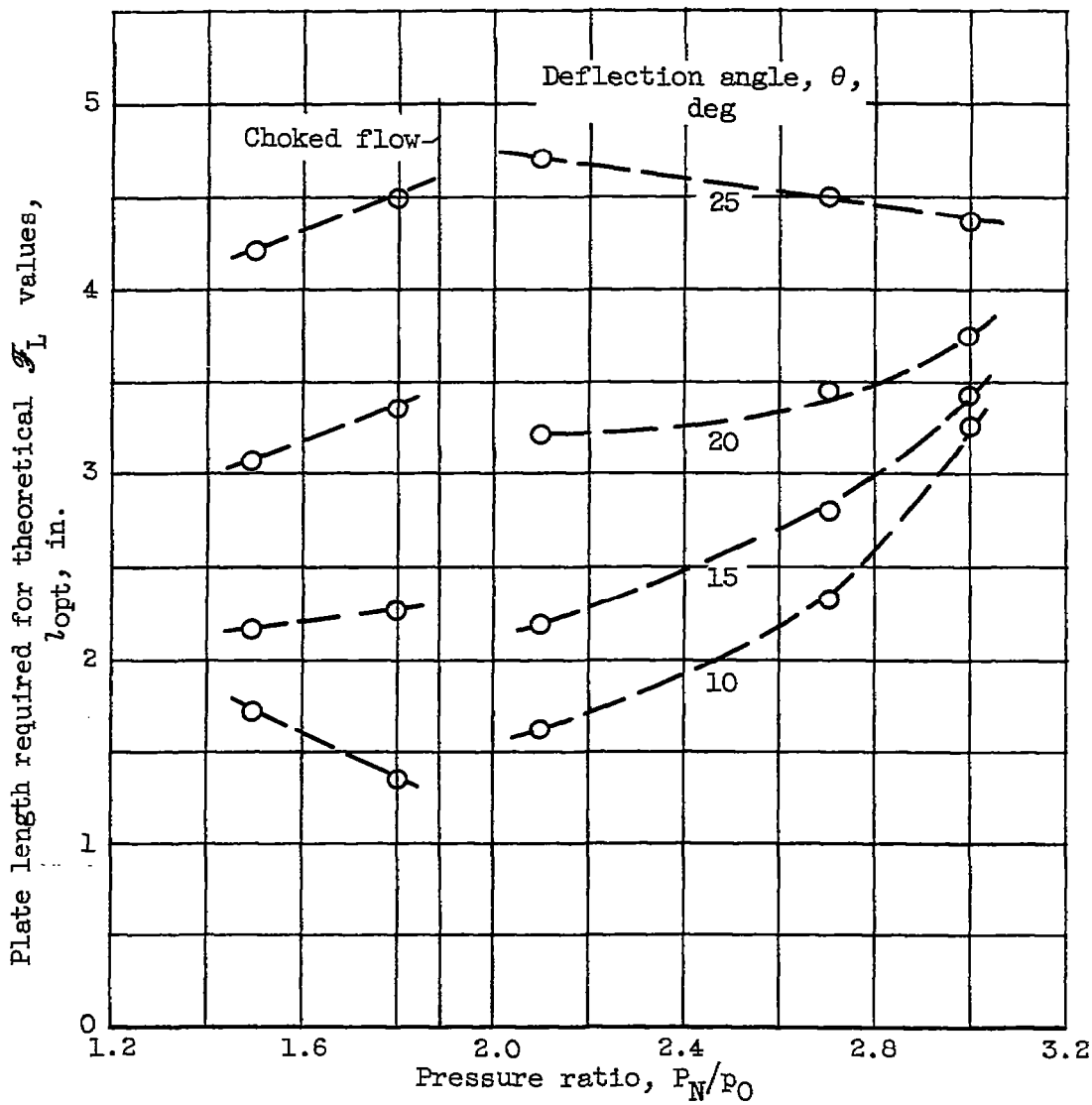

Figure 11. - Example of deflection-plate lengths calculated for achieving theoretical ratio of lift to undeflected thrust as function of pressure ratio and various deflection angles. Nozzle height, 1.5 inches.

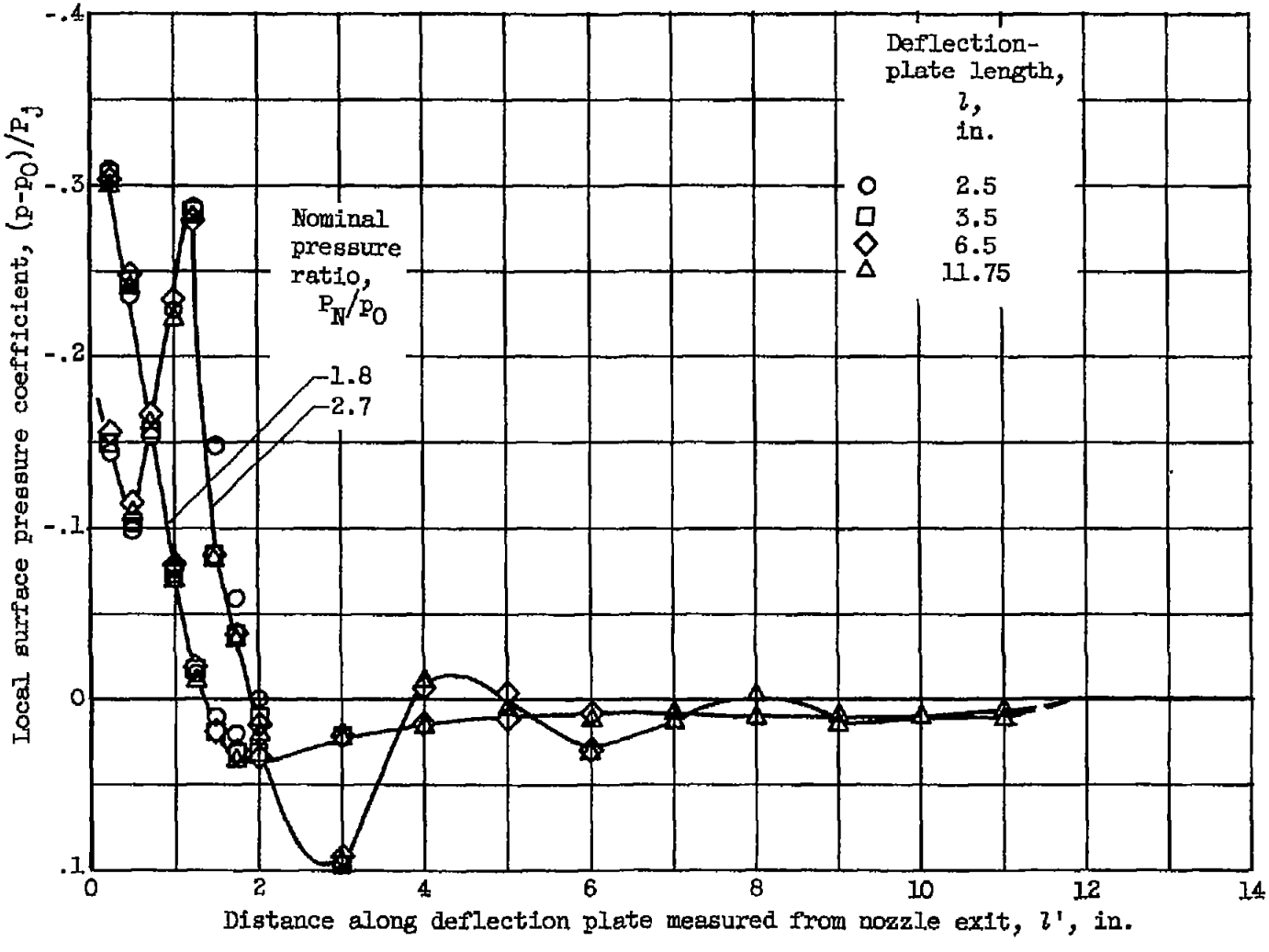

Figure 12. - Typical surface pressure distributions over deflection plate for pressure ratios below and above choking and several plate lengths. Nominal pressure ratios, 1.8 and 2.7; deflection-plate angle, 10°; nozzle height, 1.1 inches.

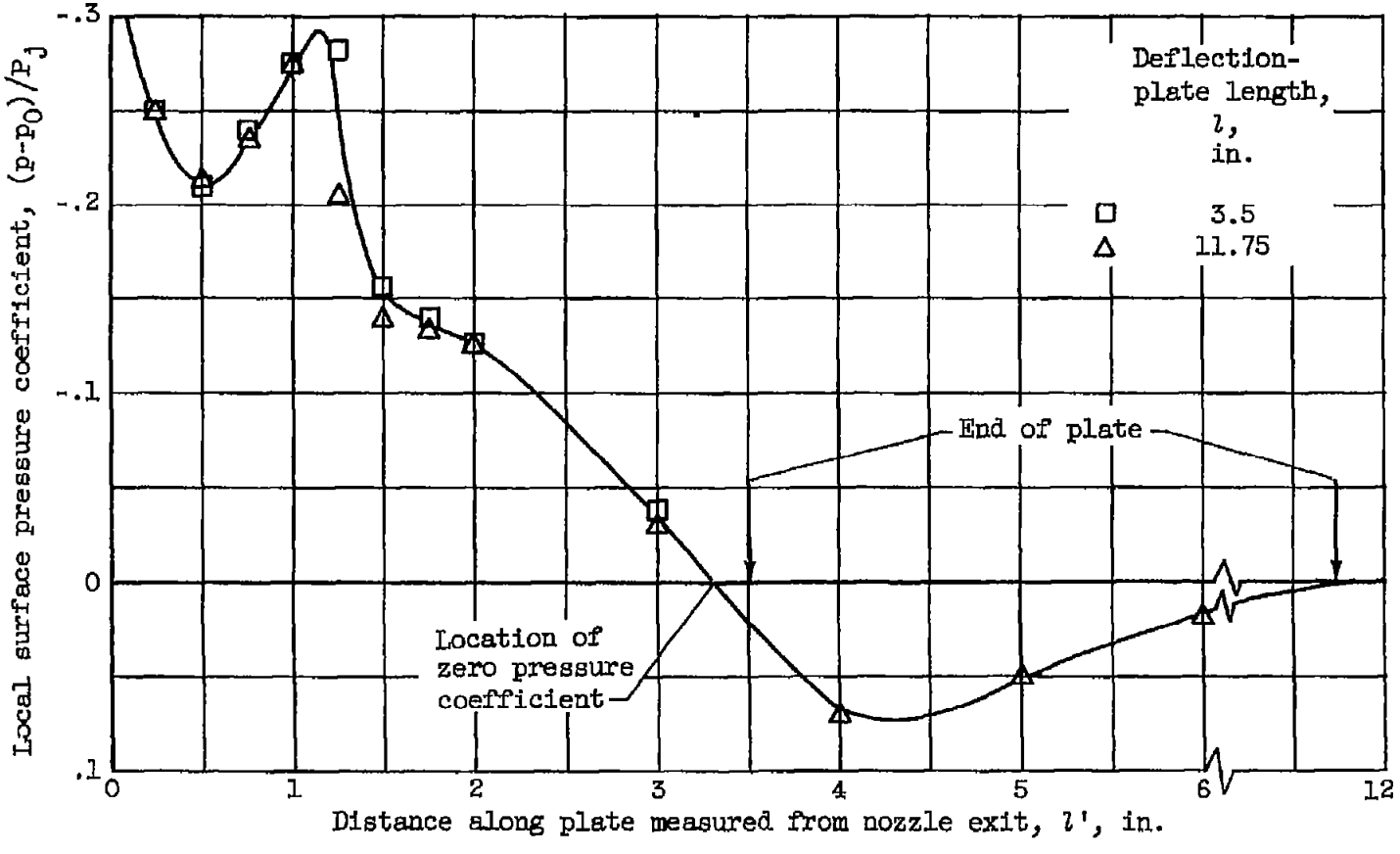

Figure 13. - Pressure distribution over 3.5- and 11.75-inch deflection plate for nozzle height of 1.1 inch, deflection angle of 20°, and nominal pressure ratio of 3.0.

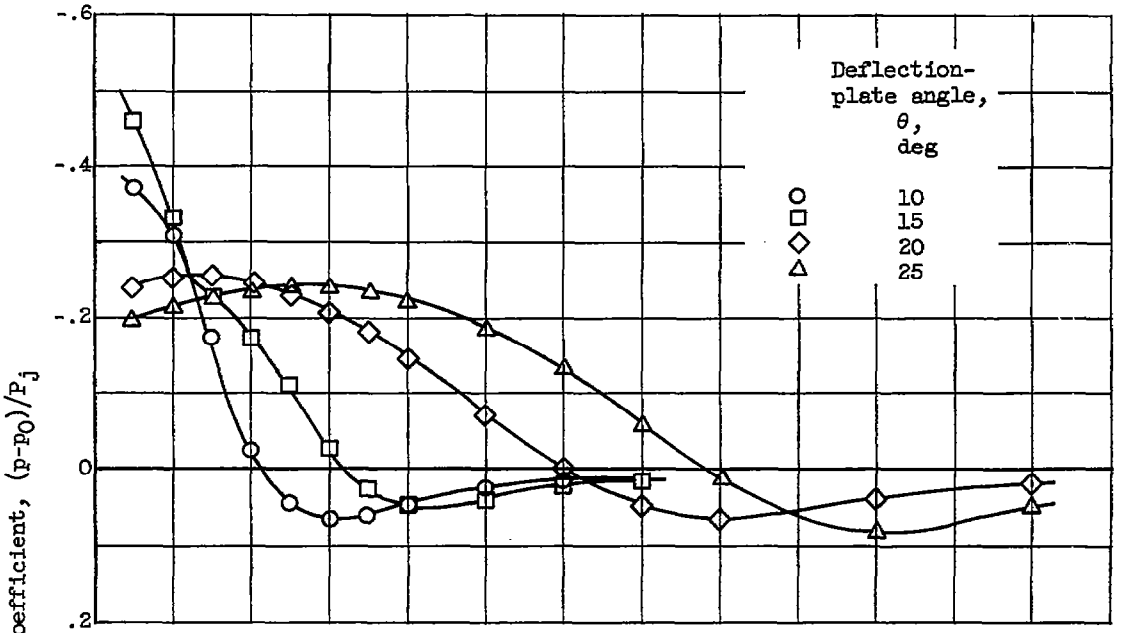

(a) Effect of deflection-plate angle on pressure distribution over plate surface. Nozzle height, 1.1 inches.

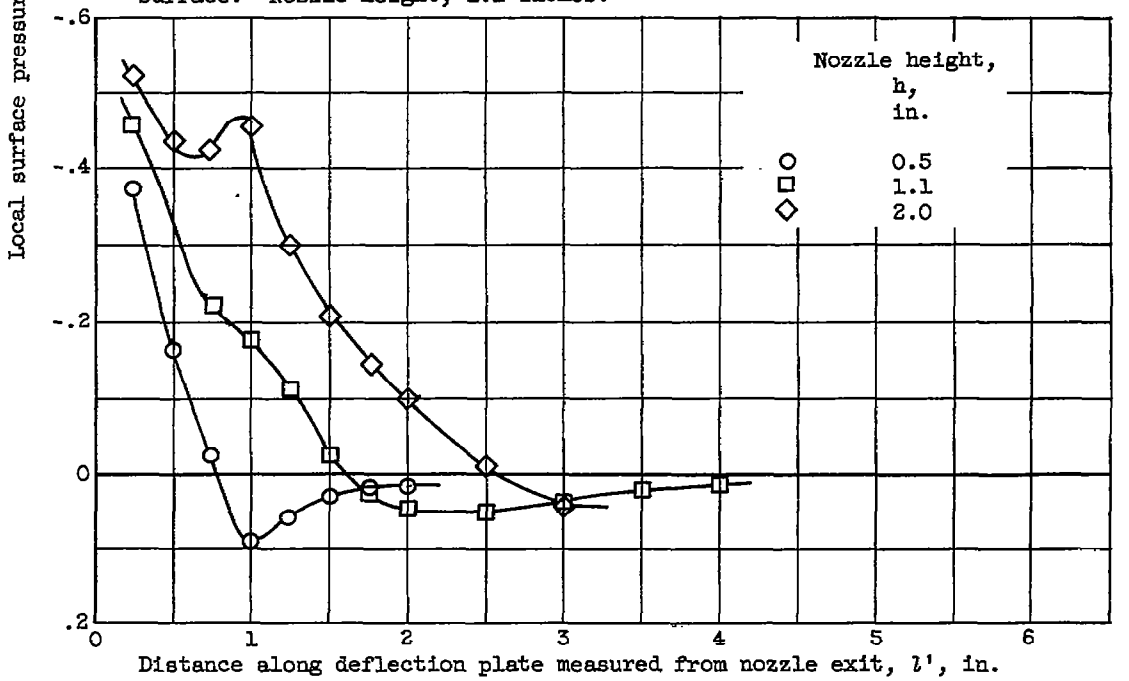

(b) Effect of nozzle height on pressure distribution over plate surface. Deflection angle, 15°.

Figure 14. - Effect of deflection-plate angle and nozzle height on surface pressure distribution. Nominal pressure ratio, 2.1; plate length, 11.75 inches.

4745

4745 CM-6 back

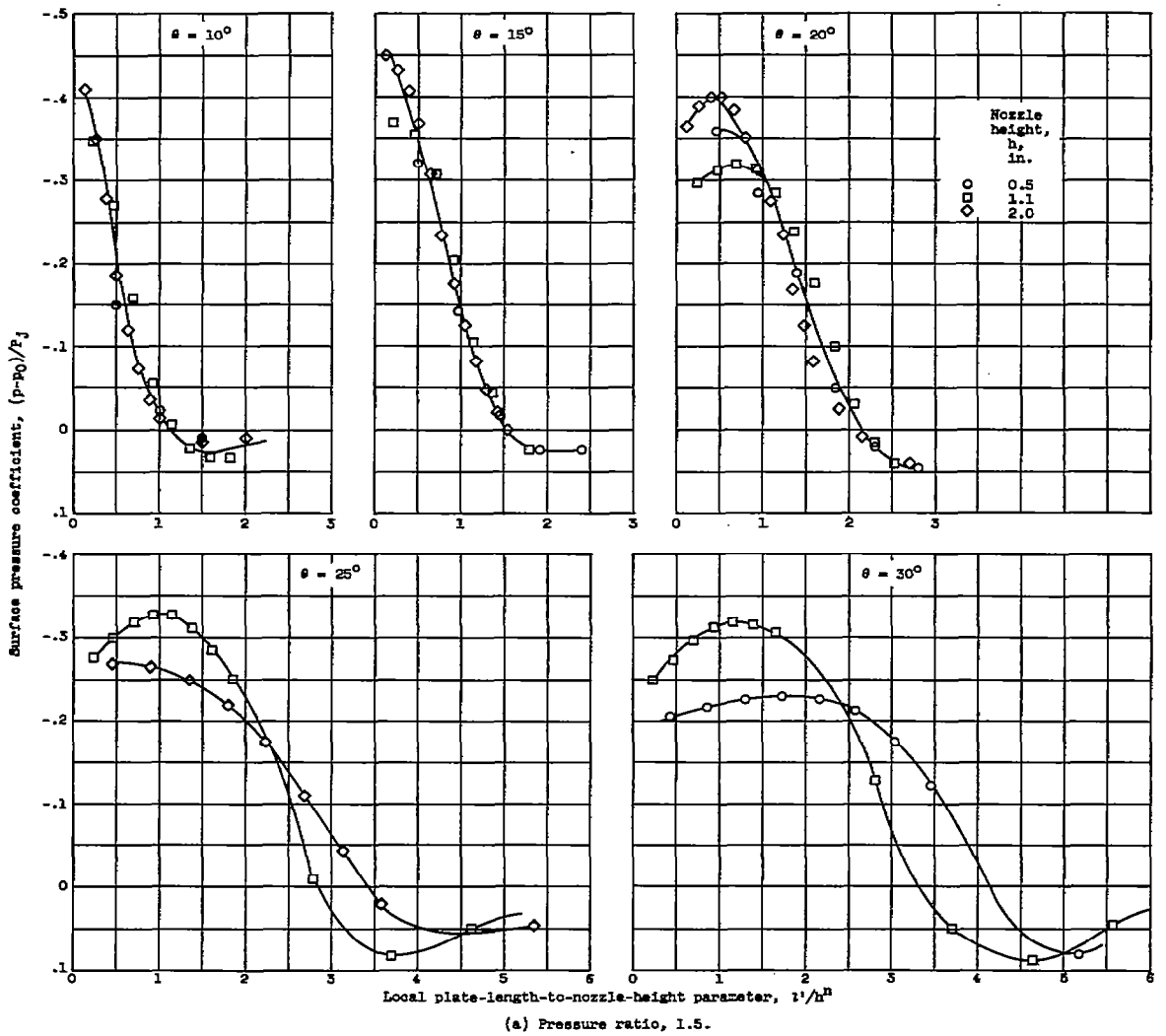

(a) Pressure ratio, 1.5.

Figure 15. - Summary of surface pressure coefficients in terms of local plate-length-to-nozzle-height parameter.

4745

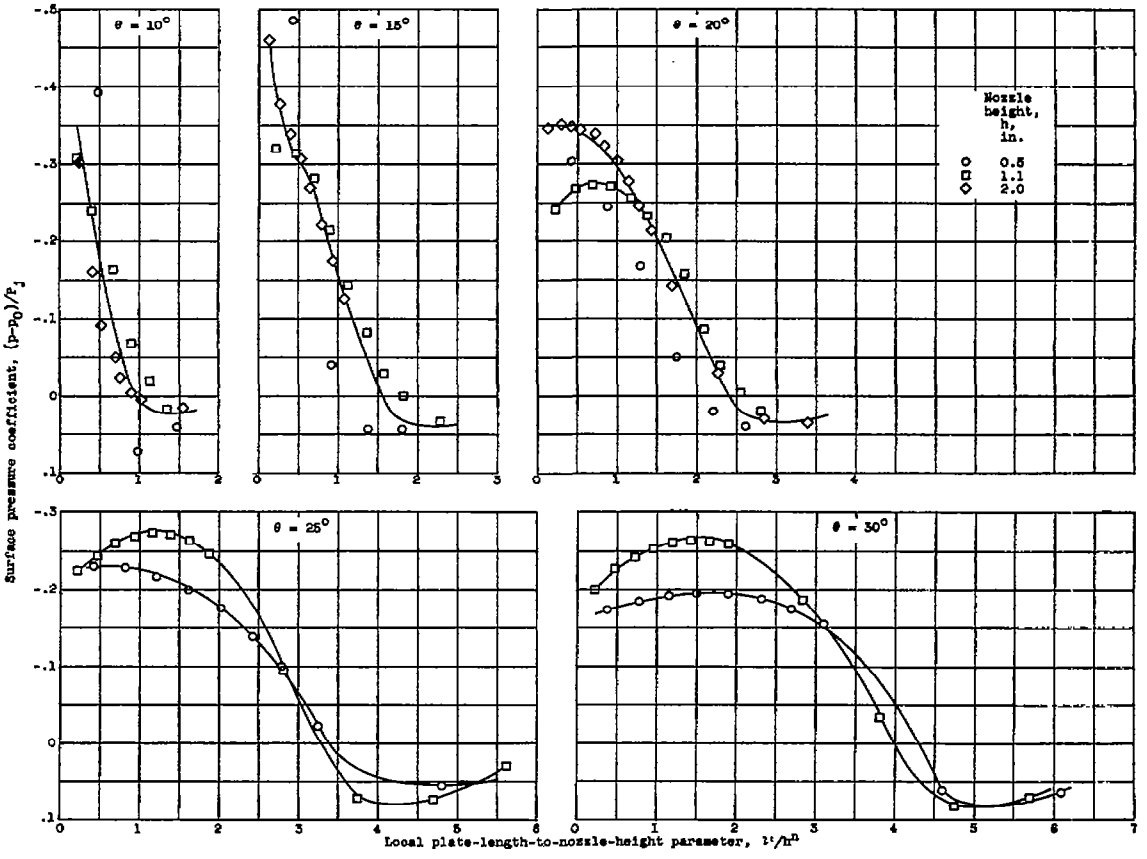

(b) Pressure ratio, 1.8.

Figure 15. - Continued. Summary of surface pressure coefficients in terms of local plate-length-to-nozzle-height parameter.

4745

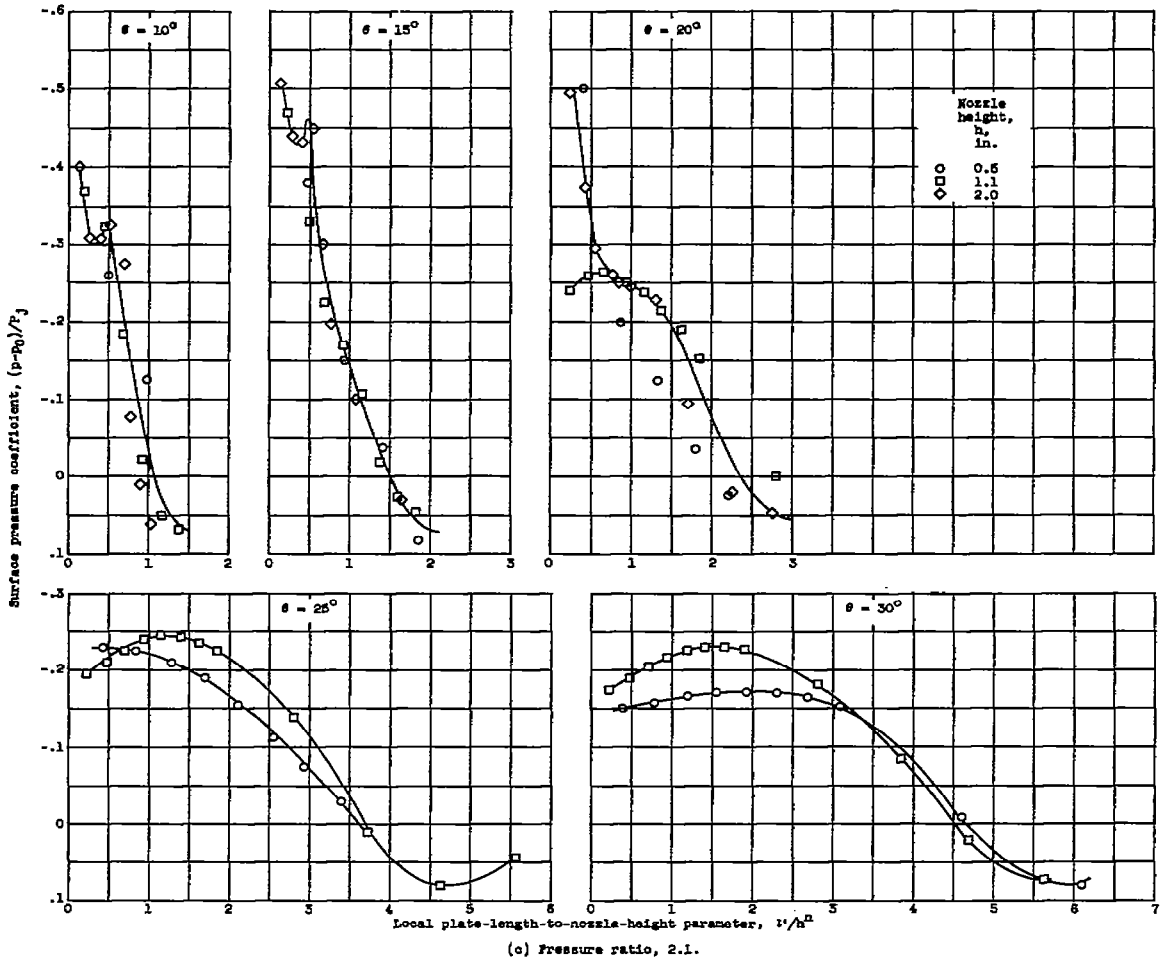

(c) Pressure ratio, 2.1.

Figure 15. - Continued. Summary of surface pressure coefficients in terms of local plate-length-to-nozzle-height parameter.

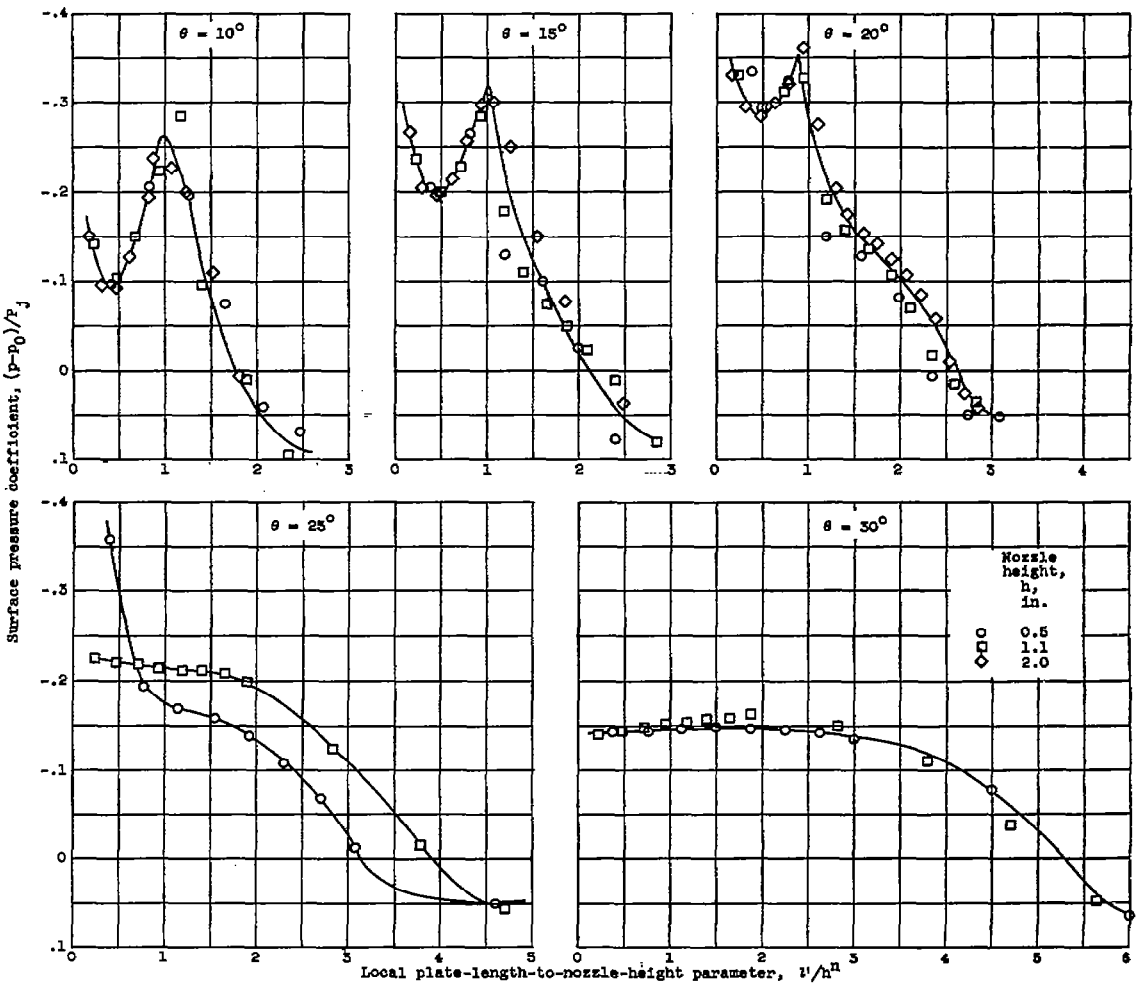

(d) Pressure ratio, 2.7.

Figure 15. - Continued. Summary of surface pressure coefficients in terms of local plate-length-to-nozzle-height parameter.

4/45

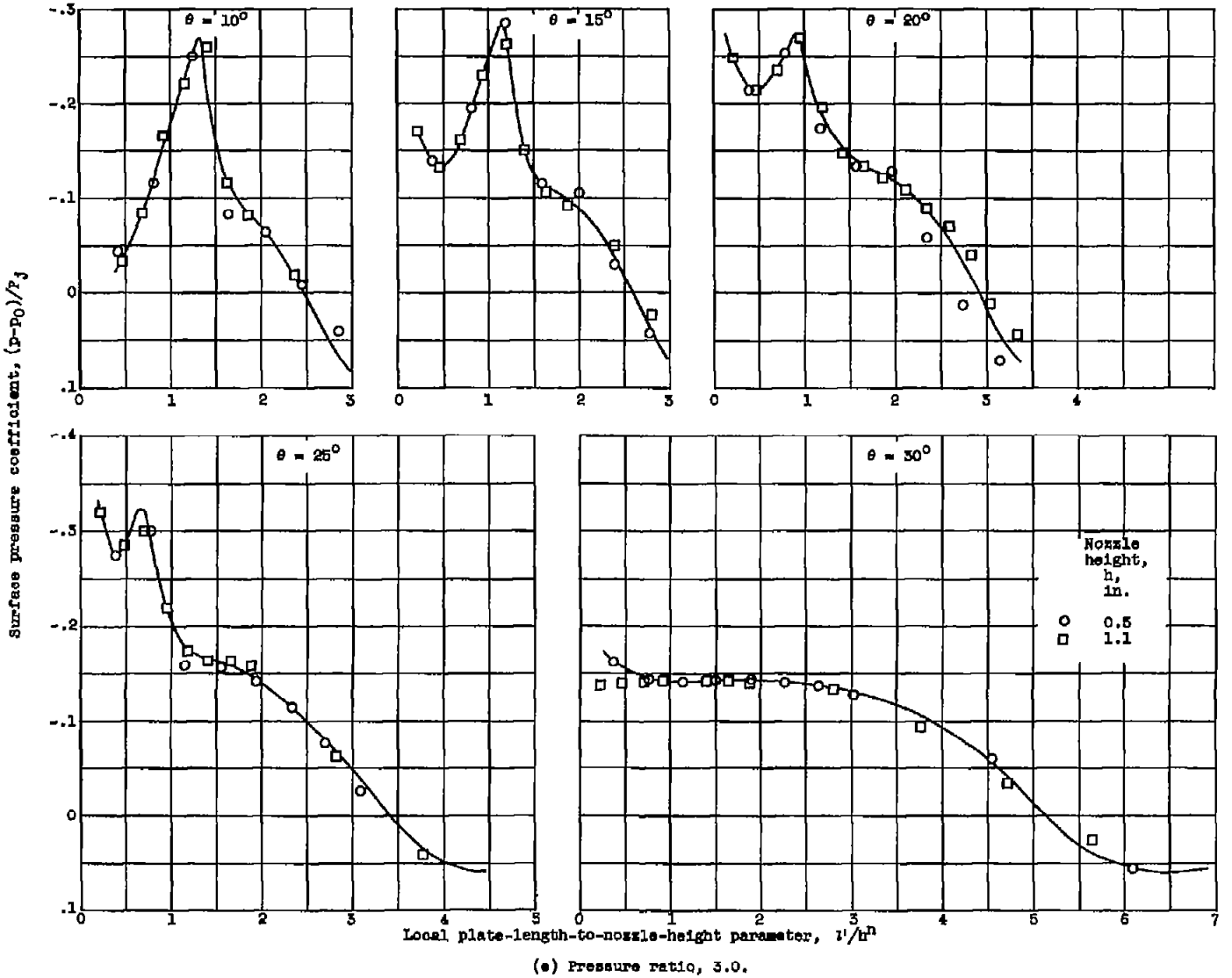

(e) Pressure ratio, 3.0.

Figure 15. - Concluded. Summary of surface pressure coefficients in terms of local plate-length-to-nozzle-height parameter.

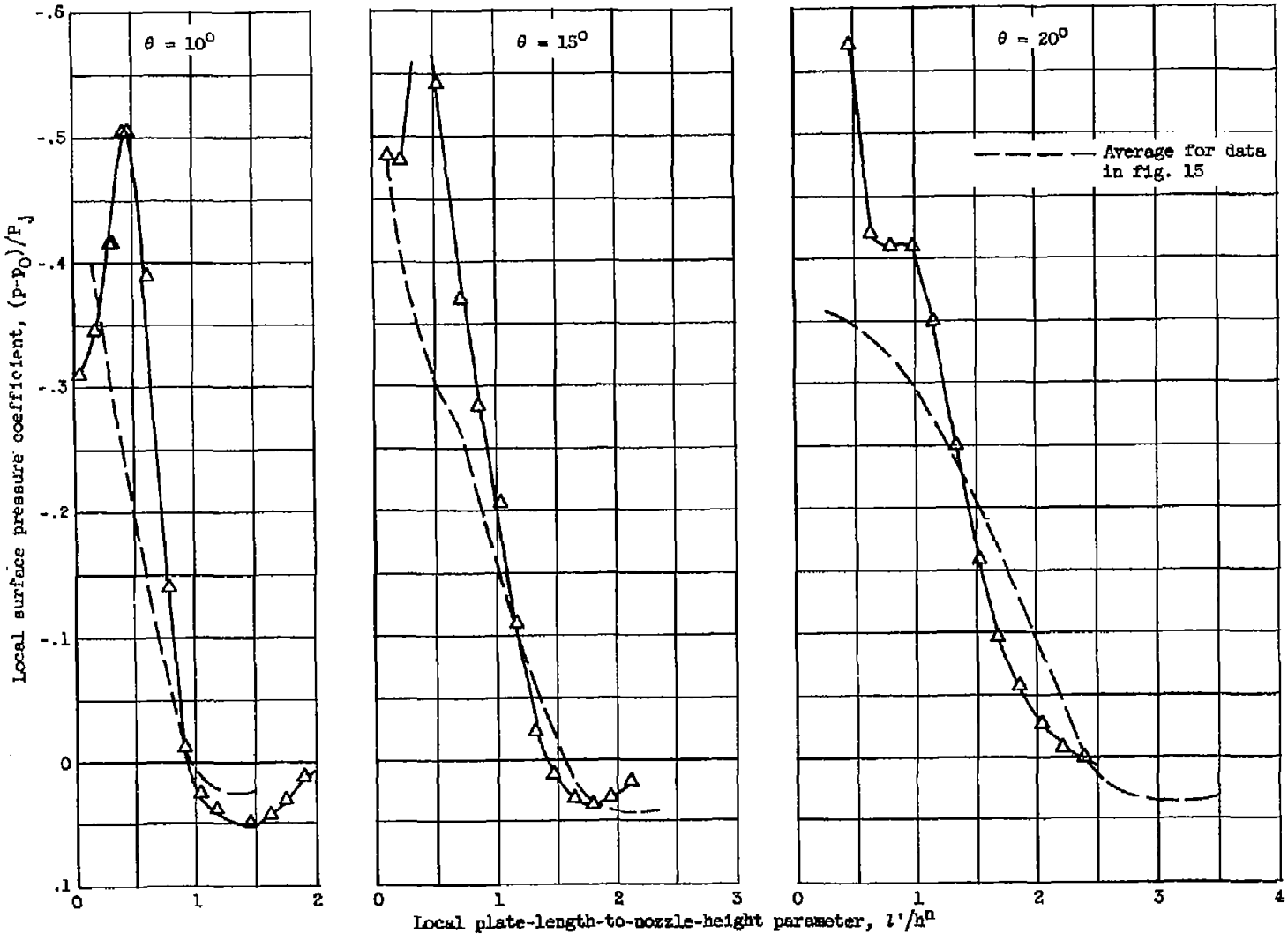

Figure 16. - Effect of nozzle contour at nozzle exit on surface pressure distribution. Nominal pressure ratio, 1.8; nozzle height, 3.7.

4745

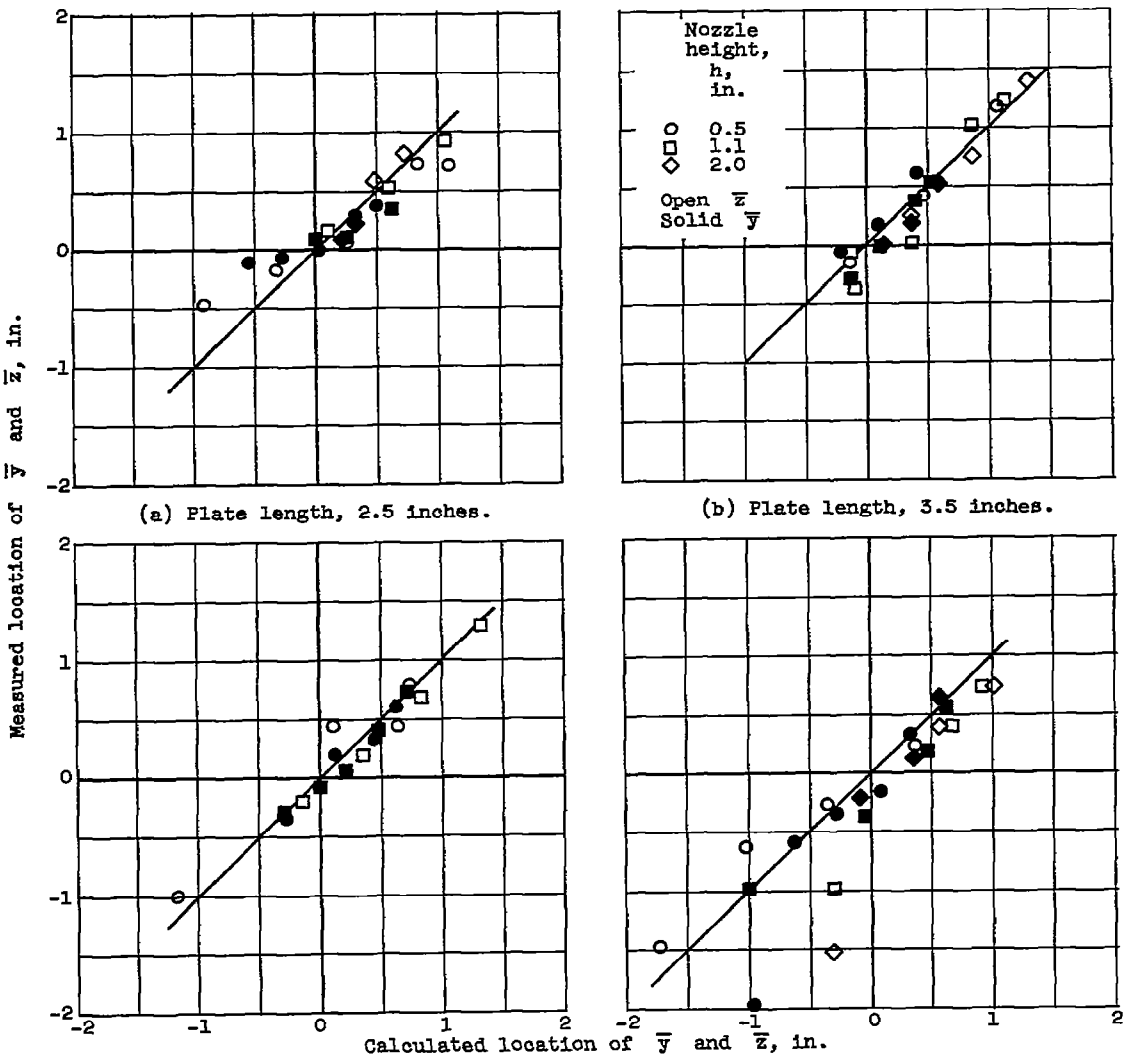

(a) Plate length, 2.5 inches.

(b) Plate length, 3.5 inches.

(c) Plate length, 6.5 inches.

(d) Plate length, 11.75 inches.

Figure 17. - Comparison of measured center-of-pressure locations with those calculated from equation (D2). Nominal pressure ratio, 2.1.